REVIEW

Check for updates

Heterojunction catalysts for CO_2–HCOOX interconversion cycles

Yu-Shuai Xu, [ID] Dong Xu, [ID] Jie-Sheng Chen [ID] and Xin-Hao Li [ID]*

Conversion of CO_2 to formic acid and/or formates (HCOOX) is a promising way to reduce carbon emissions. At the same time, HCOOX, as an excellent hydrogen storage material, can realize the safe storage and transportation of hydrogen energy. Therefore, the design of efficient catalysts for the closed-loop interconversion of CO_2 and HCOOX is an important way to achieve dynamic carbon and energy cycling. A heterojunction catalyst as a kind of typical heterogeneous catalyst has the characteristics of convenient interface adjustment, a stable structure, and easy separation, which is preferred for practical uses. Intensive progress has been made in the exploration of heterojunction-based catalysts for CO_2 hydrogenation and HCOOX decomposition reactions. This review comprehensively summarizes the recent advances in heterojunction-type catalysts for CO_2–HCOOH interconversion under different driving forces, focusing on the design of electronic effects at the interface of heterojunction catalysts, as well as the role of heterojunction catalysts in different catalytic systems.

1. Introduction

Annually increased CO_2 emission requires more sustainable techniques to capture CO_2 for not only permanent storage but also efficient transformation into valuable products.[1–3] As a cheap and harmless C1 resource, carbon dioxide could be selectively converted into feedstock chemicals and fuels, effectively reducing the dependence on petrochemicals.[4–8] Although CO_2 has already been used as a chemical feedstock in the

industrial conversion of some organic compounds, the amount of CO_2 used chemically accounts for only 1% of global CO_2.[9]

As a result, the scientific and industrial community has launched intense research activity to the exploration of more powerful paths for large-scale and/or green-energy-driven conversion of CO_2 into useful chemicals.[10–13] In recent years, the catalytic hydrogenation of CO_2 to produce a variety of value-added fuels or chemicals, including methanol, ethanol, formic acid, *etc.*, has been widely reported.[14–18] However, considering the huge gap between the amounts of CO_2 emissions and actual use,[19] the potential technologies for large-scale transfer of CO_2 to value-added chemicals are highly required.

School of Chemistry and Chemical Engineering, Frontiers Science Center for Transformative Molecules, Shanghai Jiao Tong University, Shanghai, 200240, P. R. China. E-mail: xinhaoli@sjtu.edu.cn

Yu-Shuai Xu received his BS degree in the School of Chemistry and Chemical Engineering from Northwestern Polytechnical University in 2020. Now he is a PhD candidate majoring in chemistry at Shanghai Jiao Tong University and his research interest is exploring the application of Schottky heterojunction catalysts in green conversion of small molecules.

Yu-Shuai Xu

Dong Xu received his BS degree in the School of Chemistry and Chemical Engineering from Anhui University of Technology during 2011–2015. Then, he received an ME degree from Hefei University of Technology in 2018. Now he is a PhD candidate majoring in chemistry at Shanghai Jiao Tong University and his research interest is constructing synergistic systems of binary Schottky heterojunctions and exploring their catalytic function.

Dong Xu

Several chemicals were prepared directly from the hydrogenation of carbon dioxide, including methanol, and carbon monoxide, already with relatively high consumption needs in practical use as direct fuels.[20–22] There is still huge room to further explore the potential of other products for real use. Among these products, formic acid (FA) is the one that has been proven to be converted from CO_2 in different energy-driven systems under mild conditions in favor of the practical application.[23–26] FA, as one of the basic organic chemical raw materials, has been widely used in textiles, leather, dyes, medicine, and other fields,[27,28] and even plays an important role in fuel cell technology,[29,30] of which the yield is still not satisfied the real consumption.[31,32]

As an ideal hydrogen energy carrier with a high hydrogen storage capacity (53 g L^{-1}),[33] FA is easily decomposed to release H_2 on rationally designed catalysts under mild conditions (<100 °C, ambient pressure).[34,35] Through the suitable coupling of HCOOX (X = H, Na, K, NH_4, etc.) synthesis and dehydrogenation reactions, a sustainable carbon-neutral hydrogen cycle is established for the safe and convenient storage and transportation of hydrogen,[36,37] which is the key problem in the utilization of hydrogen energy compared to traditional high-pressure gas storage methods. Therefore, the interconversion based on CO_2 and formic acid/formate is a potential way to realize the mass production of HCOOX from CO_2 reduction for reversible hydrogen storage.

To meet the need for cheaper and safer hydrogen storage techniques and reduction of CO_2 emission, the reaction of the interconversion should be extended to an applicable level. Several recent reviews have provided a comprehensive introduction to the application of different types of catalysts, including homogeneous catalysts, single-atom catalysts, and supported catalysts, in the hydrogenation of CO_2 or the decomposition of HCOOX.[38–43] However, there is a lack of a systematic discussion on the role and application of the rectifying interface effect in the heterogeneous catalysts for the CO_2–HCOOX interconversion processes, which is also a vital factor for the catalytic performance. Heterojunction catalysts with highly
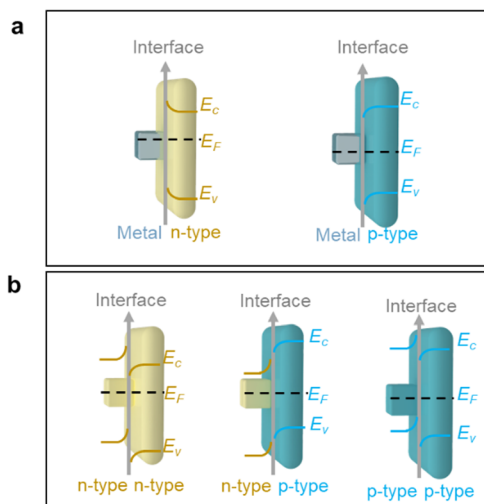

Fig. 1 Schematic of the different contact interfaces of metal–semiconductor heterojunctions (a) and semiconductor–semiconductor heterojunctions (b).

coupled rectifying interface structures and tuneable electron density at the specific interface are widely used in different system catalytic reactions.[44–47] This review summarizes the recent advances in heterojunction catalysts for CO_2–HCOOX interconversion under different catalytic systems, focusing on the roles of rectifying effects at the interface of different heterojunction catalysts in the reactions, and the potential of developing heterojunction-based catalysts for the practical applications.

2. Heterojunction-based catalysts for the CO_2–HCOOX interconversion cycles

Generally speaking, metal–semiconductor (M–S) heterojunction and semiconductor–semiconductor (S–S) heterojunction are the two main kinds of heterojunctions with rectifying

Jie-Sheng Chen

Jie-Sheng Chen is currently a professor at Shanghai Jiao Tong University (2008-present). He received his BSc (1983) and MSc (1986) degrees from Sun Yat-sen University and PhD degree (1989) from Jilin University. After work experience as a postdoctoral researcher at the Royal Institution of Great Britain in London, he returned to Jilin University in 1994. His research interest is focused on the interfacial interactions of material components and the electrochemical and catalytic performances of solid materials.

Xin-Hao Li

Xin-Hao Li is currently a professor at Shanghai JiaoTong University (2013-present). He completed each of his academic degrees from Jilin University from 1999 to 2009, receiving his PhD in 2009 with professor Jie-Sheng Chen. He then joined Prof. Markus Antonietti's group as a postdoctoral researcher at the Max-Planck Institute of Colloids and Interfaces from 2009 to 2012. His current scientific interest is mainly focused on the development of Mott–Schottky catalysts for energy and environmental science.

contacts for possible modulation in the interfacial electronic structure and thus the catalytic activity for the interconversion of CO_2 and HCOOX.[48–50] According to the different types of semiconductors, including n-type semiconductors and p-type semiconductors, the M–S heterojunction can be further divided into M-n type and M-p type heterojunctions (Fig. 1(a)).[49,51] The electronic interface will form between the metal and semiconductor, depending on the difference in work functions (φ) or Fermi levels (E_F).[51] The electrons will migrate from the part with the relatively high Fermi level to the other part until the Fermi levels on the two sides of the rectifying interface reach equilibrium. For the metal and n-type semiconductor heterojunction, the Fermi level of the metal should be lower than that of the n-type semiconductor, leading electrons to flow from the semiconductor to the metal, with the conduction and valence bands of the n-type semiconductor bending downward at the interface.[48,52] Similarly, the metal with a higher Fermi level and a p-type semiconductor heterojunction generates the electrons flowing from metal to semiconductor, with the conduction and valence bands of the p-type semiconductor bending upward at the contact interface.[52,53]

The S–S heterojunction can also be divided into n–n,[46,50,54] p–p,[47] and n–p heterojunctions,[55] according to the type of composed semiconductors.[51] Similar to the M–S heterojunctions, different S–S heterojunction types will lead to different interfacial electronic structure distributions (Fig. 1(b)), because of the discrepancy in the Fermi level of the two sides. The as-formed rectifying interfaces provide infinite possibilities for the subsequent interfacial electronic regulation of heterojunction catalysts.[46,51]

The heterogeneous structure not only retains the inherent catalytic activity of each component but also improves the performance of the active sites through the interaction in the contact interface.[1,45,56,57] The interface synergy in the heterojunction is powerful and adjustable, providing a solution for the catalysis of various reactions, including hydrogenation reaction, C–C coupling reaction, nitrogen reduction reaction, *etc.*, which has been proven to play a key role in previous studies.[44,53,57–60] The possible charge transfer between different components in heterojunction structures may result in interfacial polarization regulating the adsorption/desorption of reactants and intermediates,[45,55,61] leading to superior catalytic performance for the target products.[1,62] Taking a hydrogen evolution reaction (HER) as an example, the enriched electron density of Pt nanoparticles caused by the rectifying effect at the highly coupled heterojunction interfaces between Pt metal and Co/NC support boosts the adsorption of H^+ and H_2 release, leading to the outstanding performance with 6.9 mV *vs.* RHE at 10 mA cm^{-2} in acid.[56] Naturally, we can extend the application of heterojunction catalysts with specific active sites to CO_2–HCOOX interconversion driven by different forces, to achieve the goal of reducing CO_2 emissions and safe hydrogen use (Fig. 2). Through the suitable construction of heterojunction catalyst systems, hydrogen can be transferred into the liquid state of HCOOX by the efficient hydrogenation of CO_2 for the safe storage and transportation of hydrogen. Later, the
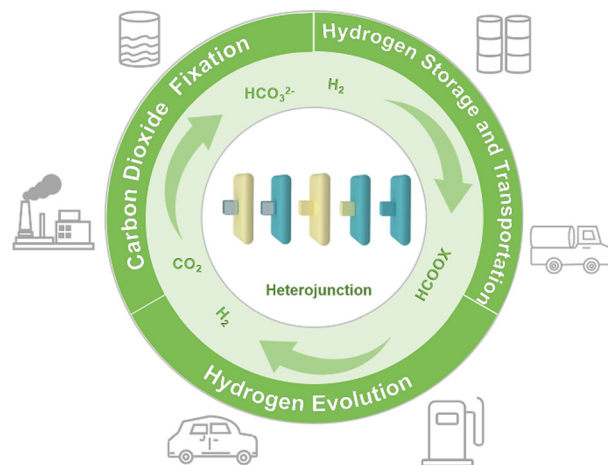

Fig. 2 Carbon-neutral HCOOX-based hydrogen cycle system on heterojunction catalysts.

hydrogen could be released by the dehydrogenation of HCOOX for the practical hydrogen energy use scenario.

3. The reaction pathways of CO_2– HCOOX interconversion cycles

In the CO_2–HCOOX loop interconversion, hydrogen could be safely stored by the hydrogenation of CO_2, and the liquid hydrogen carrier can release H_2 through the decomposition of HCOOX. It is necessary to understand the pathway of CO_2– HCOOX interconversion for the reasonable design of corresponding catalysts.

3.1 Hydrogenation of CO_2 to HCOOX

In different CO_2 hydrogenation systems, hydrogenation of CO_2 to HCOOX is considered to be the most atomically economical. However, CO_2 is a thermodynamically stable molecule with inherently low reactivity,[23,42] leading to a challenge in the hydrogenation of CO_2 to HCOOX.

The hydrogenation reaction of gas phase CO_2 to HCOOH is thermodynamically unfavorable with $\Delta G_0 = 32$ kJ mol^{-1}, as shown in Table 1.[38] The hydrogenation of CO_2 to HCOOH will be a thermodynamically favorable reaction with $\Delta G_0 = -4$ kJ mol^{-1} in the liquid system (Table 1).[38,63] However, due to the different additives in the real reaction, the substrate of the hydrogenation reaction is not actual CO_2 but rather includes carbonate, bicarbonate, carbamate, or CO_2–tertiary amine adduct.[19,38,64–66] The hydrogenation of HCO_3^- to form formate in the base additive system has a $\Delta G_0 = 0$ kJ mol^{-1}, with a thermodynamic advantage compared to the gas phase CO_2.[67] According to the reaction substrates in the hydrogenation reaction, there are two widely accepted reaction pathways,

Table 1 Reaction Gibbs energy for the reduction of CO_2/HCO_3^- to formate/formic acid

Reaction	ΔG_0 (kJ mol^{-1})
$HCO_3^- + H_2 \rightarrow HCO_2^- + H_2O$	0
$CO_2(g) + H_2(g) \rightarrow HCOOH$	32
$CO_2(aq) + H_2(aq) \rightarrow HCOOH$	−4

including CO_2 and bicarbonate reduction pathways.[32,68] In the typical thermocatalytic hydrogenation process, it is widely accepted that H_2 adsorbs on the active sites and hetero-dissociates into hydride and proton.[69] The hydride further nucleophilically attacks the carbon of the adsorbed CO_2 or HCO_3^- to form the target formate.

In the electroreduction of CO_2 to HCOOX, the reaction pathway on the tin-based catalyst is widely recognized.[70] During the reduction process, H_2, CO, and HCOOX are all possible products, with the corresponding intermediates of *H, *COOH, and *OOCH, respectively.[71–73] The key to enhancing the selectivity of HCOOX lies in promoting the production of the specific *OOCH intermediate while inhibiting the formation of *COOH, which generates byproducts such as CO.[73–75]

3.2 Decomposition of HCOOX

There are two widely accepted pathways for the decomposition of HCOOH, including the dehydrogenation (Table 2) and the dehydration (Table 2) of HCOOH, which depend on the used catalysts and reaction conditions.[76] The dehydrogenation of HCOOH with a $\Delta G_0 = -48.4$ kJ mol^{-1} to release hydrogen is the desired reaction.[77] While the dehydration of HCOOH with a $\Delta G_0 = -28.54$ kJ mol^{-1} is the not expected side reaction, producing CO that is toxic to the active sites.[76,78] Except for the two pathways from HCOOH, HCO_2^- could also be transferred to HCO_3^- by hydrogen evolution, with a nearly $\Delta G_0 = 0$ kJ mol^{-1},[67] which has no other gas evolution (Table 2).

According to recent research, three pathways of the HCOOX decomposition are generally accepted, including the formate way, the indirect way, and the carboxyl way.[79,80] The electrooxidation of HCOOX can also be divided into three pathways, the formate way, indirect way, and direct way.[79,81] In the formate way, there are generally considered to be two adsorption configurations, namely bidentate formate (*HCOO$_B$) and monodentate formate (*HCOO$_M$).[40,82] The monodentate formate (*HCOO$_M$) is generally accepted as the active intermediate for the cleavage of C–H bonds.[40,83] The selectivity and activity for the decomposition and electrooxidation of HCOOX on the catalysts mainly depend on the adsorption intermediates in the reaction pathway.

Table 2 Reaction Gibbs energy for the decomposition of formate/formic acid

Reaction	ΔG_0 (kJ mol^{-1})
$HCO_2^- + H_2O \rightarrow HCO_3^- + H_2$	0
$HCOOH \rightarrow CO_2(g) + H_2(g)$	−48.4
$HCOOH \rightarrow CO(g) + H_2O$	−28.54

4. Heterojunction catalysts for CO_2–HCOOX interconversion cycles

The HCOOX-based hydrogen storage and release performed in the thermal catalytic systems have the potential to achieve the practical use of hydrogen.[84,85] Besides the homogeneous catalyst,[63] the heterogeneous catalysts are easy to separate and reuse but limited in their activity.[38,43] Much effort has been contributed to develop efficient heterogeneous catalysts for the superior performance of the CO_2–HCOOX interconversion reaction.[86,87] A typical Pd/AC catalyst is used for the hydrogenation of CO_2 to formate, making 1 kg of H_2 storage with saturated ammonium bicarbonate in 55 bar at 293 K within 2 h (Fig. 3).[88] The Pd/AC catalyst can also be used in the dehydrogenation of HCOOX to release H_2 in the 10 M ammonium formate, producing 1 kg H_2 at 393 K in 40 min (Fig. 3), with the potential to replace the traditional hydrogenation way at the hydrogenation station.[88] Appropriate construction of the heterojunction catalyst can improve the activity and selectivity of the CO_2–HCOOX interconversion reaction.[86,89,90]

4.1 Heterojunction catalysts for the reduction of CO_2/HCO_3^- to HCOOX

The reduction of CO_2 or carbonate to formic acid and formate in thermal catalysis systems is an important way to use CO_2.[27,91] The central challenge of the reaction is devising a suitable catalyst to reduce the activation energy and change the kinetic process, given the chemical stability of CO_2.[24,92] Compared to the homogeneous catalysts which are hard to separate, heterogeneous catalysts are more in line with the principle of green chemistry and have greater economic advantages for practical application, because of their easy recovery and reuse.[43] Noble metals are widely used in hydrogenation reactions, and different methods have been applied to promote the activity and stability of noble metals, improving the utilization of noble metals.[34,41,85,93,94] The construction of hetero-structures based on noble metals is an effective path to change the surface electronic structure of the noble metals and then
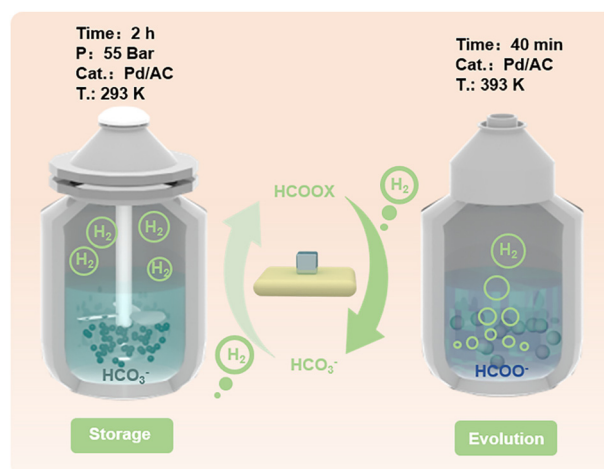
Fig. 3 The schematic of the cyclic HCO_3^- and $HCOO^-$ storage and release of 1 kg H_2 on a typical Pd/AC catalyst.

promote the activity and the stability of the active sites. In addition, the catalytic performance of non-noble metals can also be enhanced by directly constructing a heterostructure.

4.1.1 Noble metal heterojunction for the reduction of CO_2/ HCO_3^- to HCOOX. So far, heterogeneous catalysts containing noble metal (Au, Pd, Pt, *etc.*) nanoparticles or clusters have been extensively studied in the reduction of bicarbonate and carbon dioxide to formic acid/formic acid.[66,90,94,95] Among these noble metals, metal Pd with excellent H_2 adsorption capacity shows excellent hydrogenation activity compared with other transition metals, especially in the CO_2/HCO_3^- hydrogenation reaction.[27,91]

A variety of optimization methods including defects, alloys, doping, and other means were applied to further promote the performance activity of Pd-based catalysts.[9,41,93] The Pd-supported catalyst is a common type, while a suitable semiconductor not only has a support function but also forms a heterojunction structure with metals to change the electronic structure of the metal interface by interfacial electron rectifying.[96] Thus, the electronic structure at the interface of the active site plays a crucial role in the reaction process.

The key to the Pd-based heterojunction structure is the selection of supports. The catalytic performance of Pd supported on different supports ($BaSO_4$, Al_2O_3, and carbon) was investigated, and according to the research results, the Pd/C catalyst showed the best activity with a TOF value of 25 h^{-1}.[97] The carbon-based support was then highly used as the main stream for the efficient construction of Pd-based supported catalysts.[41,98] The Pd/AC catalyst gave a satisfactory turnover frequency (TOF) value of 527 h^{-1} under 2.75 MPa and 293 K.[88] The reduced graphene oxide (rGo) was also applied to construct a Pd-based supported catalyst that showed good catalytic hydrogenation performance from bicarbonates to formates.[99]

Moreover, the N-doped carbon as a support to avoid the aggregation of metal nanocrystals could form the heterojunction to stabilize metal species and tune the electronic density of the metal surface, further promoting the performance in hydrogenation of CO_2 towards formate.[93,100]

The mesoporous graphitic carbon nitride (g-C_3N_4) is also the typically functional support due to the specific band structure favored for tuning the electronic state of a metal through the interaction at the interface between the metal and support, which has the potential for facilitating CO_2 activation and hydrogenation.[43,96] A typical Pd/g-C_3N_4 catalyst with the novel mesoporous graphitic carbon nitride support shows highly enhanced performance in the hydrogenation of CO_2 to formic acid compared to the inert support and remarkable stability in the catalytic process under neutral conditions.[34]

Besides the carbon-based support, the metal oxides (TiO_2, CeO_2, ZnO, *etc.*) are also considered as potential support candidates for the construction of heterojunctions with noble metals, because of their tunable band structure and basic sites.[27,91,92] Pd/ZnO and Pd/CeO_2 as the two common metal oxide support catalysts show superior catalytic performance for the reduction of CO_2 to formate.[90] The modified electronic structure of the Pd surface caused by the interaction at the heterojunction interface and the suitable basic sites in the
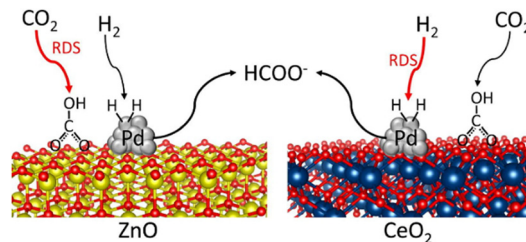

Fig. 4 Scheme of the reduction of CO_2 to $HCOO^-$ over Pd/ZnO and Pd/ CeO_2.[90] Reproduced with permission. Copyright 2019, Elsevier.

support boost the hydrogenation of CO_2 (Fig. 4), leading to high catalytic activity.

Moreover, the potential practical application of heterojunctions based on noble metals and suitable semiconductors is hindered by the high cost of the noble metals.[64]

4.1.2 Alloy heterojunctions for the reduction of CO_2/ HCO_3^- to HCOOX. Alloying is one of the most common strategies to regulate the electronic properties of metal nanoparticles by the electronegativity difference between metals.[92,93,101] Furthermore, the alloy can also realize the control of interface electrons through the construction of a heterojunction to achieve efficient hydrogenation of CO_2 and HCO_3^-. The electronic properties of noble metals play a crucial role in achieving high catalytic activity. An alloy heterojunction strategy can thus promote the utilization of noble metals.

A typical PdAg alloy supported on anatase TiO_2 is synthesized for the hydrogenation of CO_2 to formic acid, giving an outstanding reaction rate of HCOOH yield of 1429 h^{-1} (Fig. 5(a)) over the optimal sample with the Pd/Ag ratio of 5 at 40 °C.[102] The electron density of the Pd metal could be efficiently tuned by the interaction of support and the addition of Ag (Fig. 5(b)). The formation of alloys (PdAg) allows Ag to modify the electron density of Pd and enhance the utilization rate of Pd atoms, thus promoting the catalytic performance of CO_2 hydrogenation. However excessive addition of Ag inhibits the H-spillover effect on the active site of Pd metals and blocks the hydrogenation process, resulting in the degradation of catalyst performance. Therefore, the appropriate alloy ratio and the joint adjustment of the support enable the Pd–Ag alloy heterojunction material to achieve a high formic acid yield.
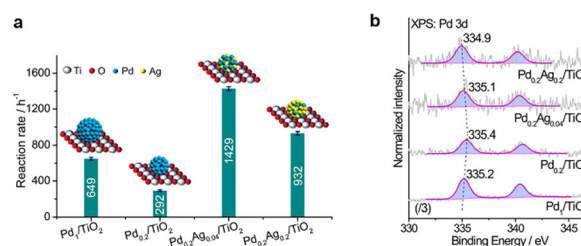

Fig. 5 (a) The reaction rate of HCOOH production (h^{-1}) calculated on various catalysts at 40 °C based on the surface Pd. (b) Quasi-*in situ* XPS spectra of Pd 3d for various Pd/TiO_2 and PdAg/TiO_2 samples. Reproduced with permission.[102] Reproduced with permission. Copyright 2023, American Chemical Society.

4.1.3 Non-noble metal heterojunction for the reduction of CO_2/HCO_3^- to HCOOX.

Pd-Based heterogeneous catalysts usually exhibit excellent activity in converting CO_2 and bicarbonate into formic acid. However, the high cost of noble metals limits their further applications. The use of a non-noble metal and support could decrease the cost of catalyst preparation and separation after the reaction.[43,64,103]

An innovative dyadic heterojunction structure composed of cheap MoC nanocrystals and nitrogen-doped carbon sheaths (MoC@NC) was designed for efficient CO_2 hydrogenation to formic acid (Fig. 6(c)), exhibiting a turnover frequency (TOF) value of 0.15 mol_{FA} mol_{MoC}^{-1} h^{-1} at 70 °C.[103] The rectifying contact between molybdenum carbide as a metallic phase and nitrogen-doped carbon support with an open band gap can significantly enhance the electron enrichment of molybdenum carbide nanoparticles. The transfer charge at the rectifying interface could be precisely adjusted by regulating the band structure of nitrogen-doped carbon supports (Fig. 6(a) and (b)), and the electron enrichment state at the interface of MoC can be effectively controlled. The electron-rich MoC and electron-deficient N-carbon support in the interface of MoC@$N_{5.6}$C could polarize the CO_2 molecule and largely promote the preadsorption of CO_2 (Fig. 6(c)). More importantly, the specific rectifying interface of the dyad can also improve the activation of CO_2 to the key intermediate *HOCO, which dominates the selectivity to target HCOOH production (Fig. 6(d)).

The heterojunction structure also controls the electronic state of the interface metal through the interfacial electronic transmission and regulates the valence state type and proportion of the active site according to the reaction demand. The formed Ni/TiO_2 heterojunction structure at the interface causes the change of the electronic state at the Ni interface and the electron flow to the support, making the ratio of Ni^0 and Ni^{2+} within the appropriate range, thus realizing the cooperative catalysis of Ni^0 and Ni^{2+}, and promoting the catalytic performance of the hydrogenation of carbonates to formic acid.[64] At the same time, the presence of the TiO_2 support also enhances the stability of the chemical state of the metal in the reaction process.

4.2 Heterojunction catalysts for the dehydrogenation of HCOOX

Noble metal nanoparticles (Au, Pd, Pt, etc.) have been investigated for the decomposition of formate with promising catalytic activities under relatively mild conditions.[35,77,78,104] However, the unwanted dehydration reactions to produce CO often occur on noble metal catalysts, reducing the catalytic activity and selectivity.[89] To overcome this problem, different methods have been developed, including the optimization of size, shape, electronic structure, alloy, and so on.[35,77,105] Among these methods, the construction of heterojunctions with metals and suitable semiconductor supports is identified as an efficient way to modify the electronic structure of the metal surface for the high dehydrogenation of FA.[106,107] On the other hand, the bimetallic nanoparticles with alloy structures are considered more CO-tolerant for the dehydrogenation of formate.[104] Therefore, alloying and heterostructures could be combined to form alloy-type metal and support heterostructures to achieve multi-component control for the promising performance of the dehydrogenation of formate.

4.2.1 Noble metal heterojunction for the dehydrogenation of HCOOX.

The noble metal supported catalysts with suitable cheap supports inhibit the agglomeration of metal nanocrystals and construct efficient heterogeneous catalysts for practical applications,[76,89] which is confirmed to have a significant effect on the catalytic performance of the loaded metals. The typical heterojunction structure of the metal and the support can form the specific interface with the electron transfer between the two parts, leading to the change in the interfacial electronic structure of the metal nanocrystals, which further improves the catalytic activity and selectivity for the HCOOX dehydrogenation. Different supports (oxides, carbon, g-C_3N_4, etc.) are used in the construction of noble metal-based heterojunctions to enhance the catalytic performance of the metal.[89,104,106]

Common nitrogen-doped carbon (NCs) materials as supports and stabilizers provide uniformly dispersed Pd NPs and strong electron effects, thus enhancing the catalytic performance of HCOOX dehydrogenation.[106] A typical Pd nanoparticles@g-C_3N_4/SiO_2 successfully synthesized by a sol–gel method exhibits an extraordinary hydrogen production rate from formic acid (Fig. 7(a)). The band structure of carbon nitride can be simply tuned by changing the condensation temperature, further controlling the electron density of the Pd metal at the interface through the interface rectifying effect. With the gradually enlarged band gap of CN/SiO_2, the electronic density of embedded Pd nanoparticles becomes more enriched. There is also a positive correlation between Pd enrichment and catalytic activity (Fig. 7(b)), confirming that the regulation of the electron density of the metal by a heterojunction improves the reaction activity of formic acid decomposition.
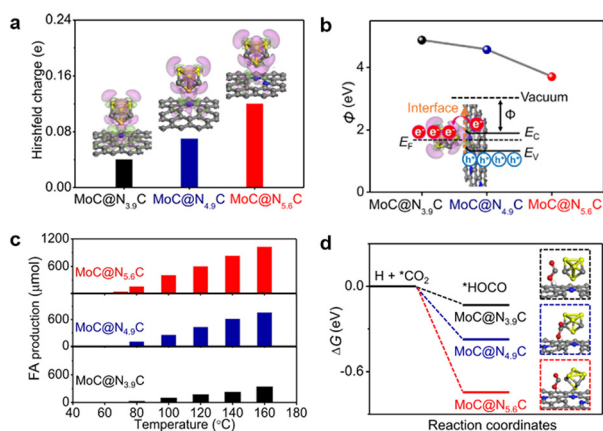

Fig. 6 (a) The Hirshfeld charge transferred to the d-MoC cluster from N_xC supports. (b) The work functions (φ) measured by ultraviolet photoelectron spectroscopy (UPS) of the samples. (c) The production of HCOOH over various MoC@N_xC catalysts at different temperatures. (d) The calculated Gibbs free energy diagram for the reduction of *CO_2 to *HOCO at the various MoC@N_xC heterojunctions.[103] Reproduced with permission. Copyright 2020, Elsevier.
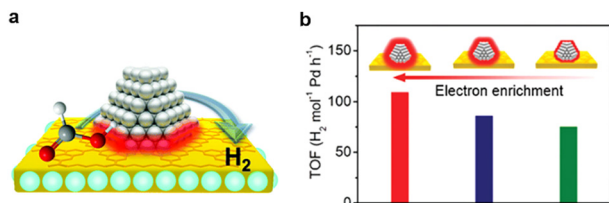
Fig. 7 (a) The scheme of the interface electron redistribution between Pd and supports caused by the Mott–Schottky effect. (b) The turnover frequency (TOF) values for the dehydrogenation of HCOOH of Pd@CN/SiO$_2$ catalysts.[106] Reproduced with permission. Copyright 2016, The Royal Society of Chemistry.

Fig. 9 The schematic for the synthesis process of Pd–WO$_x$/(P)NPCC, Pd/(P)NPCC, and Pd–WO$_x$/NPCC NCs used for the dehydrogenation of HCOOH.[107] Reproduced with permission. Copyright 2022, Elsevier.

The electronic effect between the semiconductor and the metal has been confirmed that could improve the activity of the heterojunction catalysts. On this basis, the pore structure of the semiconductor can be further designed to achieve more exposed metal active sites, promoting catalytic performance.[89,108]

An N-doped porous carbon driven by the carbonization of the typical metal–organic framework is used as an efficient support for the construction of a Pd@CN900K catalyst with Pd nanoparticles.[108] The as-designed Pd supported on the porous N-doped carbon catalyst shows an outstanding performance of the dehydrogenation of HCOOH with a turnover frequency (TOF) value of 14 400 h^{-1} at 60 °C (Fig. 8(a) and (b)). Based on the N-doped carbon as a stabilizer for the electron donor, Pd^{2+} can be stabilized on the support and further reduced into ultrafine nanoparticles, which is beneficial for the reaction. The interaction between the Pd nanoparticles and the N-doped carbon leads to the change in the electronic state of the active sites, facilitating the breakage of the C–H bonds in the formic acid considered as the rate-determining step.

The construction of multiple heterostructures is also a path that can be explored for the efficient dehydrogenation of HCOOX. Pd–WO$_x$ nano-heterostructures anchored on a phosphate-modified nitrogen-doped porous carbon cage (NPCC) driven by the ZIF-8@ZIF-67 core–shell present an outstanding FA dehydrogenation catalytic performance with 100% H$_2$ selectivity (Fig. 9).[107] Besides phosphate-modified NPCC as an electron donor transports electrons to the Pd–WO$_x$ heterojunction through the strong metal–support interaction (SMSI) effect. Additionally, the rectifying contact promotes electron transfer from WO$_x$ supports to the Pd metal, redistributing electrons at the Pd–WO$_x$ interface and

resulting in electron-rich Pd nanocrystals. The enhanced electron density of Pd can further promote the formate adsorption performance, resulting in better catalytic activity.

4.2.2 Alloy heterojunction for the dehydrogenation of HCOOX. Meanwhile, optimizing the work function of the metal components based on the alloying effect facilitates enhancing rectifying contact to accelerate the electron transfer between metal and semiconductor, thereby further improving the activity and utilization of the precious metal active site.[104,105,109]

A novel heterojunction catalyst AuPd/BNNFs-A composed of boron nitride nanofibers (BNNFs) with amine groups and AuPd alloy nanoparticles (Fig. 10(a)) is applied for the efficient dehydrogenation of HCOOH, giving an outstanding turnover frequency (TOF) value and low activation energy of 1181.1 h^{-1} and 20.1 kJ mol^{-1} without any additives (Fig. 10(c)).[109] The high distribution of the small-size AuPd alloy nanoparticles leads to an abundant interface between alloy and support with charge transfer, further modulating the electronic structure of Pd confirmed by the experiment results (Fig. 10(b)). The alloy structure also significantly influences the electronic structure of Pd, benefiting the dehydrogenation of formic acid. On the
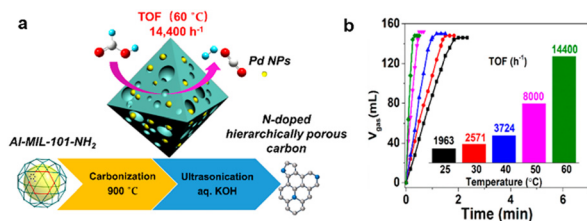

Fig. 8 (a) The schematic for the fabrication of Pd@CN900K used for the dehydrogenation of HCOOH. (b) The gas evolution and turnover frequency (TOF) values of the dehydrogenation of HCOOH over Pd@CN900K catalyst at different temperatures.[108] Reproduced with permission. Copyright 2018, American Chemical Society.
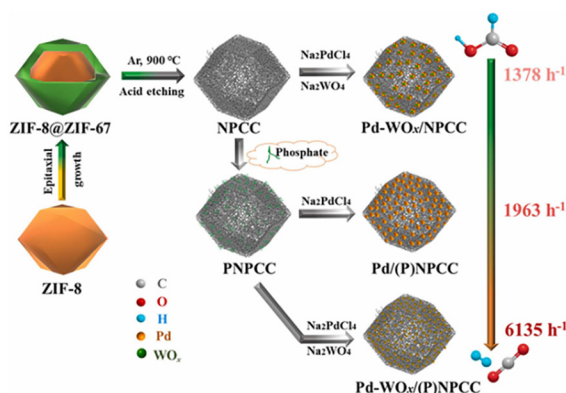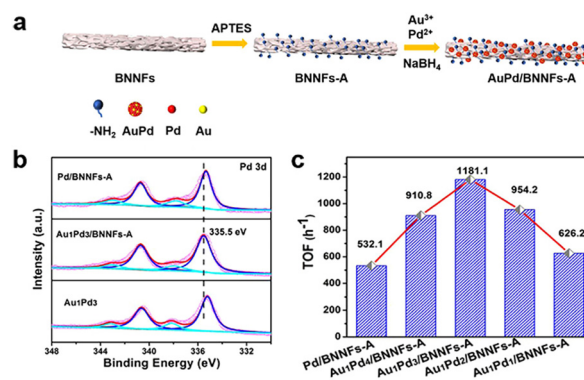

Fig. 10 (a) The schematic of the synthesis process of AuPd/BNNFs-A. (b) The X-ray photoelectron spectroscopy spectra of Pd 3d in three different samples. (c) The corresponding turnover frequency (TOF) values over various catalysts in an ambient atmosphere and at 298 K.[109] Reproduced with permission. Copyright 2021, American Chemical Society.

basis of the suitable alloy nanostructure, the special hetero-junction interface of Au$_1$Pd$_3$/BNNFs-A, and the synergistic effect of the support, the catalyst achieves excellent catalytic performance.

4.3 Heterojunction catalysts for interconversion of CO$_2$/HCO$_3^-$-HCOOX

Through the suitable construction of heterojunction catalysts, efficient storage and release of H$_2$ can be achieved by the superior hydrogenation of CO$_2$ to HCOOX and dehydrogenation of HCOOX. The noble metal shows activity for both reactions in the CO$_2$–HCOOX interconversion cycle. A Ru-based homogeneous catalyst is developed for the HCO$_2$Na-based reversible hydrogen cycle but it is limited by the reuse and regeneration of the catalysts.[33] While the heterojunction catalysts based on the noble metal overcome the drawback and also exhibit high performance.[88,100]

A Pd nanoparticle supported on the graphitic carbon nitride (Pd/mpg-C$_3$N$_4$) is confirmed to achieve HCOOX-based chemical hydrogen storage, giving a high turnover frequency (TOF) value of 144 h^{-1} without any additive at room temperature in the dehydrogenation of HCOOH and satisfactory performance for the regeneration of HCOOH by hydrogenation of CO$_2$.[110] The interaction between Pd nanoparticles and the mpg-C$_3$N$_4$ interface results in uniform nanoparticle size and further improves the performance of the CO$_2$–HCOOX interconversion.

A visible HCOOX-based hydrogen storage system is constructed over the novel Pd nanoparticles dispersed on the nitrogen-doped mesoporous carbon (Pd/NMC) catalyst (Fig. 11).[100] The electron-enriched Pd nanoparticles are formed by the rectifying contact in the interface between Pd and nitrogen-doped mesoporous carbon, which have been confirmed to be the key to promoting the bicarbonate/formate interconversion cycle.

The high-performance heterojunction catalyst in CO$_2$–HCOOX interconversion cycles has the potential to achieve a reversible hydrogen cycle for practical use in the industry, which could replace high-pressure hydrogen storage.

5. Heterojunction catalysts for electrocatalytic CO$_2$–HCOOX interconversion cycles

Electrocatalytic reduction of CO$_2$ to liquid chemicals is an interesting way for CO$_2$ fixation through the storage of electricity and hydrogen.[111,112] HCOOX, as the simplest 2e$^-$ liquid product in the electrocatalytic carbon dioxide reduction reaction (ECO$_2$RR), is a promising product to make a profit, which has not only high energy and hydrogen density but also wide applications in different yields.[73,113] As an ideal energy and hydrogen carrier, HCOOX can be directly utilized in the direct formic acid fuel cells through the formate electro-oxidation reactions (FAOR)[40] or used for dehydrogenation to release hydrogen. But the latter way in an electrocatalytic system is rarely investigated, because the electrolysis of water is the main means of electrochemical hydrogen production. Therefore,
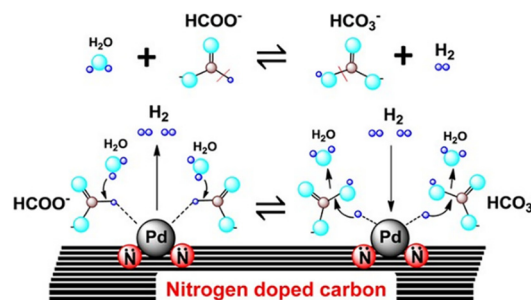

Fig. 11 The schematic of the HCOO$^-$–HCO$_3^-$ interconversion reaction process over Pd/NMC.[100] Reproduced with permission. Copyright 2016, Wiley VCH.

coupling ECO$_2$RR to formate and FAOR is considered as one of the potential pathways to achieve dynamic energy and hydrogen storage and conversion in the context of carbon neutrality.[114] To achieve the goal in the practical application scenario, an efficient and stable catalyst is a vital part. Heterojunction catalysts are widely used for the two reactions, because of the tunable electronic state of the active site by the interaction interface, which promotes the adsorption of the key intermediates and further improves the activity and selectivity of the target product.[115,116] A typical heterojunction catalyst Sn–Cu/SnO$_x$ is used for the electrocatalytic reduction of CO$_2$ to HCOOX, giving a superior HCOOX product rate of 6.8 mmol h^{-1} cm^{-2} at j_{HCOOH} of 357.9 mA cm^{-2} (Fig. 12).[117] The Pd@SnO$_2$-NSs/C with hetero-junction structure applied in the FAOR reaction exhibits satisfactory mass activities of 4.96 A mg^{-1} (Fig. 12).[118] The results suggest a high potential for the use of heterojunction catalysts for the electrocatalytic CO$_2$–HCOOX interconversion.

5.1 Heterojunction catalysts for electroreduction of CO$_2$ to HCOOX

Recently, a variety of metals (Bi, Sn, Pb, Pd, Ag, Zn, Cd, In, *etc.*) and their corresponding metal oxides/sulfides/nitrides have been used as efficient electrocatalysts for hydrogenation reduction of CO$_2$/HCO$_3^-$ to formate.[73,114,116,119,120] Some metals (Pd, Pb, Hg, and Cd) show better electrocatalytic performance in converting CO$_2$/HCO$_3^-$ to formate but are limited in practical application due to their scarcity, high cost, and toxicity. Among all the catalysts investigated to date, In-based electrocatalysts with excellent selectivity toward targeted formate and non-toxicity have attracted much attention.[121] Sn and Bi metals, as the low-cost, low-toxic, and earth-abundant metal elements, show high selectivity to formic acid and a high activity during the electrocatalytic CO$_2$ reduction reaction.[120,122] Therefore, Sn-, Bi-, and In-based catalysts are promising candidates for large-scale real-world use, because of their merits of low price, abundance, and environmental benignancy, compared to the noble metals Au, Pd, and Ag, as well as the toxic metals Pb, Hg, and Cd.

Different schemes are used to improve the catalytic performance of these three metals, in which the catalytic activity and selectivity can be greatly improved by constructing heterojunction structures. Coupling the heterostructure interfaces in the
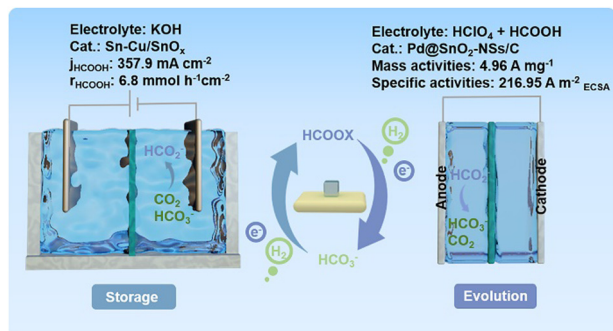
Fig. 12 The schematic of the electrocatalytic cyclic CO_2/HCO_3^- and $HCOO^-$ for storage and release of H_2 and energy.
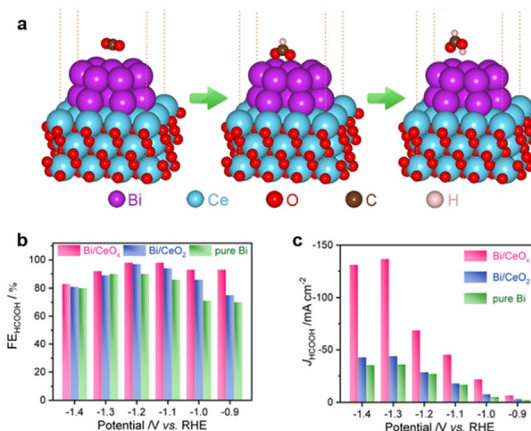

Fig. 13 (a) The pathway for the reduction of CO_2 to HCOOH over Bi/CeO_2. (b) Faraday efficiency (FE), and (c) partial current density of formic acid on the three samples at different potentials.[123] Reproduced with permission. Copyright 2021, Wiley VCH.

heterojunction could regulate the electronic structure and coordination environment of the metal-based part and then decrease the energy barriers of the key intermediates in the ECO_2RR reaction. Therefore, it is highly necessary to promote electron transfer and key intermediate adsorption on the heterojunction catalysts to perfect the ECO_2RR performance.

5.1.1 Metal–semiconductor heterojunctions for electroreduction of CO_2 to HCOOX. Through the selection of a suitable semiconductor support, a metal–semiconductor heterojunction interface is formed, and the electronic structure of the metal surface can be regulated through the electron transfer of the interface, thus promoting the adsorption of substrates and key intermediates and improving the activity and selectivity of the reaction.

As common semiconductor supports, metal oxides (BiO_2, TiO_2, CeO_2, etc.) are ideal support candidates and have shown excellent results in the research.[122–124]

A novel Bi/BiO_2 Mott–Schottky heterostructure was designed by transforming the as-synthesized Bi_2O_3/BiO_2 heterojunction during the reaction process.[124] Based on the heterogenous interface, the Bi/BiO_2 catalyst shows enhanced performance of the absorption for CO_2 and key *OCHO intermediates, leading to the outstanding selectivity (faradaic efficiency (FE) > 95%) of the target product formate in a wide potential range, accompanied by a high current density of 111.42 mA cm^{-2}.

The synthesized Bi/CeO_x catalyst by the *in situ* electroreduction of $Bi_2O_2CO_3/CeO_x$ displays high selectivity of formate with the FE (92%) (Fig. 13(b)) at a high current density of 149 mA cm^{-2} (Fig. 13(c)) and outstanding stability with a long time test of 34 h.[123] The introduction of CeO_x to form Bi/CeO_x heterostructures promotes charge transport, leading to a better performance of the adsorption and activation of CO_2, enhancing the adsorption of key intermediates *HCOO (Fig. 13(a)), further resulting in high activity and selectivity. At the same time, the formation of a heterojunction promotes the formation of much smaller particle size Bi active sites, which is also the important reason for improving catalytic performance.

In addition to oxides, carbon materials are also a common class of semiconductor supports and are widely used to design efficient metal–semiconductor heterojunction catalysts.[125,126]

A Sn/CN synthesized by reducing Sn^{2+} to metallic Sn particles in the polymeric carbon nitride (CN), with strong interaction between the Sn and CN heterostructure interface (Fig. 14(a)), exhibits good performance for durable, efficient, and highly selective electroreduction of CO_2 to formic acid (Fig. 14(b) and (c)).[126] In the stable heterojunction interface of the composite Sn/CN catalyst, electrons are transferred from the CN to the Sn atom, leading to the electron-rich structure of Sn, promoting the adsorption and activation of CO_2 molecules, thus enhancing the electroreduction of CO_2 to formate.

A novel metal In nanoparticle anchoring on a PEDOT-modified carbon (PC) heterojunction catalyst is designed by transforming In_2O_3/PC during the reaction process of ECO_2RR to formate. In_2O_3/PC presents an outstanding electrocatalytic selectivity for formate with an FE of 95.4%, an extremely high formate current density of 239.8 mA cm^{-2} at −1.18 V *vs.* RHE, and a high stability for 75 h continuous electrolysis test.[121] There are strong interface electronic interactions between In metal and PC in the In/PC heterojunction confirmed by both
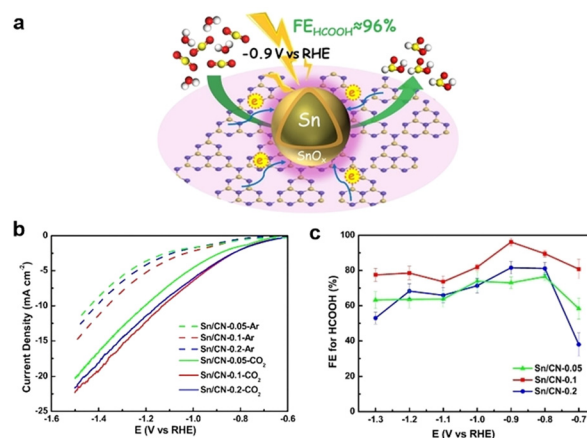

Fig. 14 (a) Schematic illustration of Sn/CN. (b) LSV curves over different electrodes in 0.1 M $KHCO_3$ electrolytes saturated with Ar (dashed line) and CO (solid line). (c) FE_{HCOOH} over different electrodes at potentials ranging from −0.7 to −1.3 V *vs.* RHE.[126] Reproduced with permission. Copyright 2020, Wiley VCH.

experiments and DFT results, elevating the p-band center of In metal active sites to the Fermi level, resulting in the lower formation energies of the *OCHO, which is the key intermediate for converting CO_2 to the target production formate.

The electronic structure of the non-noble metal surface could be tuned by the construction of a reasonable metal–semiconductor heterojunction to promote the adsorption of CO_2 and target intermediates, thus improving the performance of electrocatalysis from CO_2 to formic acid.

5.1.2 Semiconductor–semiconductor heterojunctions for electroreduction of CO_2 to HCOOX. In addition to metals, for oxides and nitrides of these metals the construction of heterojunctions is also an effective method for improving the activity, selectivity, and stability of catalysts for the ECO_2RR reaction.[116,121,125] The construction of semiconductor–semiconductor heterojunctions will also form electron transfer at the interface to achieve changes in the electronic structure of the active sites, thereby promoting the adsorption of substrates and key intermediates, further improving catalytic activity and selectivity.

A typical heterojunction structure composed of 0D SnO_2 nanodots confined on 2D graphitic carbon nitride (g-C_3N_4) nanosheets is synthesized for the electrocatalytic reduction of CO_2 to formate (Fig. 15(a)), exhibiting the superior activity (Fig. 15(c)), stability, and high selectivity to formate with an FE of 91.7% at -0.88 V $vs.$ RHE (Fig. 15(b)).[120] The abundant heterojunction interface of the highly distributed SnO_2 on the 2D g-C_3N_4 leads to a strong interaction between the two parts, resulting in efficient electron transfer from g-C_3N_4 to SnO_2, demonstrated by both the experimental and theoretical results. And electronic modulations induced by the substantial heterojunction interface were confirmed to benefit the stability of SnO_2 NDs and enhance the electroactivity of SnO_2 to achieve high selectivity to formate and low energy barriers.
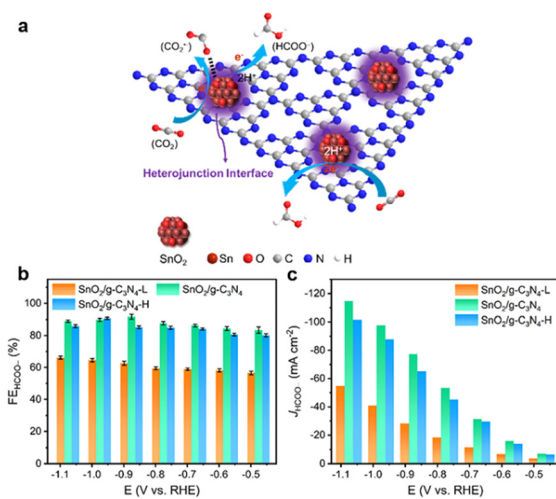

Fig. 15 (a) Schematic illustration of SnO_2/g-C_3N_4. (b) FE_{HCOO^-}, and (c) J_{HCOO^-} over the catalysts in 1.0 M KOH.[120] Reproduced with permission. Copyright 2023, American Chemical Society.

An In_2O_3/InN heterojunction is also constructed for electrocatalytic reduction of CO_2 to formate, which shows high selectivity for formate with faradaic efficiency (95.7% at -1.48 V $vs.$ RHE) and superior stability.[116] Electron transfer at the In_2O_3–InN interface enriches the InN surface with electrons, promoting substrate activation, *HCOO intermediate adsorption, and reducing the energy barrier for CO_2 hydrogenation.

Constructing semiconductor–semiconductor heterostructures could improve electron transport at the interface, enhance the selectivity of key intermediates, and achieve high Faraday efficiency and current density in the reaction.

5.2 Heterojunction catalysts for electrocatalytic oxidation of formic acid

The electrocatalytic formic acid oxidation reaction (FAOR) plays an indispensable role in the conversion and utilization of chemical energy, which is used for the anode of the direct formic acid fuel cell (DFAFC).[115]

Noble metal-based nanocatalysts (NCs) (Pt, Pd, Ru, $etc.$) are widely used for the formic acid oxidation reaction.[81,118,127] Pt-based catalysts are confirmed beneficial for the kinetics of FAOR, but are limited by the production of CO, which is unfavorable to the noble metals. Pd-based catalysts are more inclined to dehydrogenation reaction rather than dehydration to produce CO like Pt-based catalysts, which have been widely used for FAOR.[128] However, a significant challenge remains in simultaneously promoting the catalytic activity and inhibiting CO production from Pd-based catalysts. Although controlling the exposure of specific interfaces is considered to be an effective way to improve the activity and selectivity of electrocatalytic reactions, regulating the surface electronic state of the active site is also a powerful method. Through the selection of suitable materials to form a heterojunction interface with Pd, the electronic state of the Pd surface can be effectively changed. Then, the adsorption energy and selectivity of the intermediates on the surface of Pd can be regulated, which can improve the activity and selectivity of the reaction.

A Pd/NrGO@SiO$_2$ heterojunction composed of ultrasmall size Pd nanoclusters, silica layers, and the nitrogen-doped reduced GO, with a specific structure, exhibits outstanding activity for the FAOR of the peak current density (2.37 A mg^{-1}), which is significantly higher than Pd/C and Pd/rGO.[115] The typical Pd/NrGO@SiO$_2$ catalyst also shows better stability of catalytic performance with only 5% degradation of the original mass activity after the 1000 cycle tests, compared to the 100% loss of Pd/C, 61.5% loss of Pd/rGO, and 73.2% loss of Pd/NrGO. This excellent performance in the formic acid oxidation reaction of Pd/NrGO@SiO$_2$ can be attributed to the small size of Pd, the strong interactions in the interface between Pd nanoclusters and N-doped rGO, and the stabilization of the silica layer. Among these reasons, the strong interactions in the interface lead to electron-enrichment of the Pd nanoclusters, which weakens the adsorption of the unexpected CO_{ads} on the surface of Pd nanoclusters and further enhances the activity of FAOR.

Typical Pd nanosheets decorated with SnO_2 nanoflakes (Pd@SnO$_2$-NSs/C) are synthesized for formic acid oxidation

reactions with superior performance.[118] There is a strong interaction between Pd nanosheets and SnO_2 nanosheets with charge transfer, demonstrated by the X-ray photoelectron spectroscopy results. Both Sn and Pd in the Pd@SnO_2-NSs/C exhibit an obvious peak shift compared with the pure Pd nanosheets and SnO_2 nanosheets. The electronic states slightly decrease in the d-band centre of Pd, resulting in promoted adsorption of surface species. The change in the electronic structure of the interface enhances the formate pathway on the Pd surface of Pd@SnO_2-NSs/C. The lower activation energy barriers for each step of formic acid oxidation than the initial Pd (111) surface facilitate the conversion of $HCOO_B^*$ into $HCOO_M^*$, enhancing the catalytic activity of the reaction and inhibiting CO production.

Rational design and adjustment of the electrocatalyst structure by constructing heterojunction structures is an ideal strategy for exploring high-performance formic acid oxidation catalysts. To increase the current density and reduce the overpotential of electrooxidation of formic acid, both thermodynamics and kinetics must be taken into account.[40] In addition, investigations on effective non-noble metal heterojunction electrocatalysts are significant for large-scale practical applications.

6. Heterojunction catalysts for photocatalytic CO_2–HCOOX interconversion cycles

Solar energy as a clean and inexhaustible energy source is considered the ideal energy to drive the interconversion of CO_2–HCOOX.[17,129] Therefore, the development of efficient solar-chemical energy conversion systems and the delicate design of highly active and selective photocatalysts have become research hotspots in this field.[11,130] As shown in Fig. 16, the typical heterojunction Cu_2O–Pt/SiC/IrO_2 catalyst exhibits a superior HCOOX production rate of 896.6 μmol g^{-1} h^{-1} with H_2 and energy storage.[131] On the other hand, the novel heterojunction g-CN/MnO_2/MnOOH–PdAg presents a high turnover frequency (TOF) of 3919 h^{-1} for the photocatalytic HCOOX dehydrogenation to release H_2.[132] The heterojunction catalysts with rectifying contacts for the efficient photo-driven interconversion of CO_2/HCO_3^- and HCOOX exhibit an attractive prospect for practical hydrogen application.

6.1 Heterojunction catalysts for photoreduction of CO_2 to HCOOX

A solar-driven process is a potential alternative for converting CO_2 to formate instead of the traditional high-pressure and temperature energy-intensive conditions to achieve large-scale application with the lowest energy consumption.[50,133] Photocatalytic CO_2 reduction approaches can be categorized into heterogeneous and homogeneous processes. For practical applications, earth-abundant heterogeneous photocatalysts are preferred. These heterogeneous photocatalysts generally suffer from low efficiency and poor selectivity, leading to limited performance of the photocatalytic CO_2 reduction to
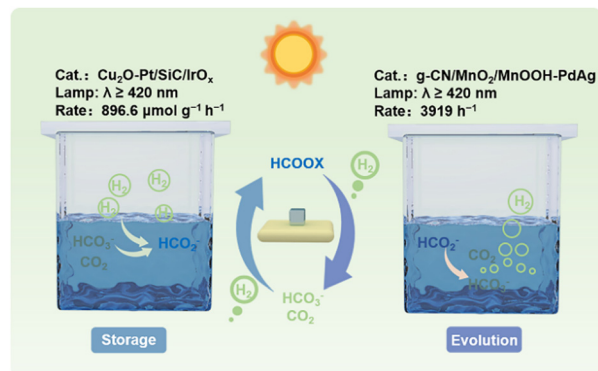

Fig. 16 The schematic of the photocatalytic cyclic CO_2/HCO_3^- and $HCOO^-$ for storage and release of H_2 and energy.

formate.[25] The construction of metal (cocatalyst) and semiconductor heterojunctions is a common method to enhance photochemical catalytic activity. Semiconductor–semiconductor heterojunctions are also an efficient way to improve the efficiency and selectivity of photocatalysts.

6.1.1 Metal–semiconductor heterojunctions for photoreduction of CO_2 to HCOOX. Photocatalytic semiconductors (TiO_2, ZnO, SiC, and CdS, *etc.*) are widely applied as catalysts for the photoconversion of CO_2 to formate upon light illumination,[131,133–135] because of the appropriate band structure, superior chemical stability, low toxicity, and the abundance amount. The single photocatalytic semiconductor always exhibits unsatisfactory selectivity and catalytic activity. Transition metals (Cu, Au, Pt, Ag, or Pd) are the commonly used active sites with high activity and selectivity in the reaction of reducing CO_2 to formate.[24,65,66] Thus, coupling transition metal as a cocatalyst and the semiconductor material into a heterojunction catalyst is expected to be an efficient way to achieve high light utilization, catalytic activity, and selectivity.

As shown in Fig. 17, a typical Pd metal can form a heterojunction with two different semiconductors (n-type and p-type), constructing the photocatalyst system. Due to the difference in the work function (φ) between the metal and the semiconductor, a rectifying contact and a Schottky barrier are formed in the interface, leading to an electron transfer.[135] What's more, the interface forms an internal electric field to drive electrons to migrate from the inside to the surface of the semiconductor, allowing photogenerated electrons and holes to separate. Due to the Schottky barrier, electron redistribution is achieved at
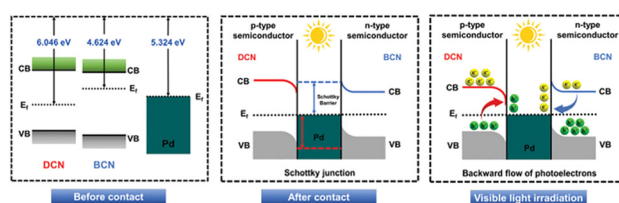

Fig. 17 The proposed scheme of charge transfer between Pd and two typical semiconductors under illumination.[135] Reproduced with permission. Copyright 2023, Wiley VCH.

the interface between Pd and semiconductor. At the Pd/n-type semiconductor interface, electrons are transferred from the conduction band (CB) of the semiconductor to the metal. An opposite flow direction of electrons is shown in the Pd/p-type semiconductor interface, and the holes in the valence band (VB) of the semiconductor are transferred to the metal. This is the typical metal cocatalyst and semiconductor heterojunction photocatalyst working mechanism under light.

The Pt-nanodots (NDs) as cocatalysts in the typical photocatalyst system Pt@TiO_2–Au nanoparticles (NPs) have robust structure and stability for efficient photoconversion of CO_2 to HCOOH, exhibiting a superior performance of 3.12% conversion rate for chemical yield from CO_2 to HCOOH and 1.84% of quantum yield.[136] The use of PtNDs as a cocatalyst significantly enhances the utilization of photogenerated electrons and CO_2 photoconversion efficiency compared to TiO_2–AuNPs under visible light. Due to the specific cocatalyst and semiconductor heterojunction structure, outstanding activity could be achieved.

The noble metals used as cocatalysts show satisfactory performance but are limited by high cost and scarcity. The non-noble metals (Ni, Co, Cu, *etc.*) are also applied for the hydrogenation of CO_2 but exhibit a gap compared to the noble metal catalysts.[17,25,134] In comparison, the alloy-based non-noble metals with specific structures can achieve a comparable activity with the noble metals for the construction of heterojunctions.

The heterojunction catalyst constructed from the NiB alloy and the In_2O_3 semiconductor is designed for the photocatalytic reduction of CO_2 to formate, giving a superior performance for the production of HCOOH (5158.0 μmol g^{-1} h^{-1}) under sunlight (Fig. 18).[137] The abundant heterojunction interfaces provided by the high distribution of the amorphous NiB alloy on In_2O_3 lead to the fast transfer of photoelectrons generated by the semiconductor In_2O_3 to NiB, inhibiting the recombination of photoelectron–hole, further efficiently promoting the quantum efficiency. And the electron-enriched NiB amorphous alloy improves the photocatalytic hydrogenation of CO_2 to formate.

Photoelectrochemical (PEC) CO_2 reduction reaction (CO_2RR) using renewable electricity and solar energy to produce value-added products selectively is also a promising long-term solution.[25,138] Different semiconductors (III–V semiconductors, metal oxides, silicon materials, *etc.*) have been investigated as the photocathodes for the PEC CO_2 reduction,[17,139,140] since the PEC CO_2 reduction was first proposed by Halmann in 1978.[141] The efficiency of the photocathodes is still a central challenge. Heterojunctions combined with semiconductors and cocatalysts
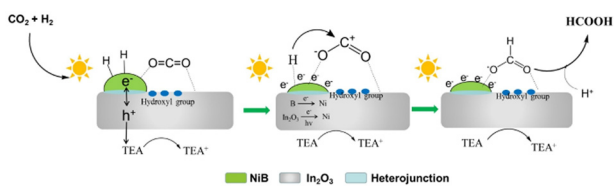
as photoelectrodes are also an efficient way to improve the performance of photoelectrochemical CO_2 reduction. The appropriate construction of the heterojunction as a photoelectrode could improve light absorption, boost charge transfer, inhibit the recombination of photogenerated electron–hole pairs, and further promote the performance of photoelectrochemical CO_2 reduction to HCOOX. A range of metals (Bi, Sn, Ag, In, *etc.*) have been used as co-catalysts to construct heterojunction photoelectrodes with semiconductors to achieve efficient photoelectrochemical reduction of CO_2 to HCOOX.[17,142–144]

An optimized Bi/GaN/Si heterojunction photocathode is developed for the reduction of CO_2 to HCOOH, giving an outstanding faradaic efficiency of formic acid (98%) at 0.3 V *vs.* RHE with 1-sun illumination.[17] The specific electronic interaction between the Bi nanoparticles and GaN nanowires at the coupled interface boosts the electron transfer to Bi nanoparticles from GaN nanowires and favors the reduction of CO_2 to HCOOH.

The heterojunction structure of semiconductor and metal enhances the separation of the photogenerated charge and improves the catalytic activity of the cocatalyst metal.

6.1.2 Semiconductor–semiconductor heterojunctions for photoreduction of CO_2 to HCOOX. The semiconductor–semiconductor heterojunction with favorable band alignment is also an efficient way for photogenerated charge separation.[51] And among the several types of heterojunctions, the Z-scheme heterojunction with the staggered gap of two n-type semiconductors has a high charge separation efficiency and superior redox ability.[11,50]

In a typical Z-scheme architecture PCN-222/CsPbBr$_3$ hybrid, photogenerated electrons in the PCN-222 with a more positive conduction band (CB) position will be injected into the valence band (VB) of another part CsPbBr$_3$ with a more negative position (Fig. 19(a)).[145] The as-designed direct Z-scheme heterojunction of PCN-222/CsPbBr$_3$ is used for the efficient photoreduction of CO_2 to formic acid, giving high enhancement in

Fig. 18 Proposed scheme of the conversion CO_2 to formate process on the NiB/In_2O_3 heterojunction under illumination.[137] Reproduced with permission. Copyright 2021, Elsevier.
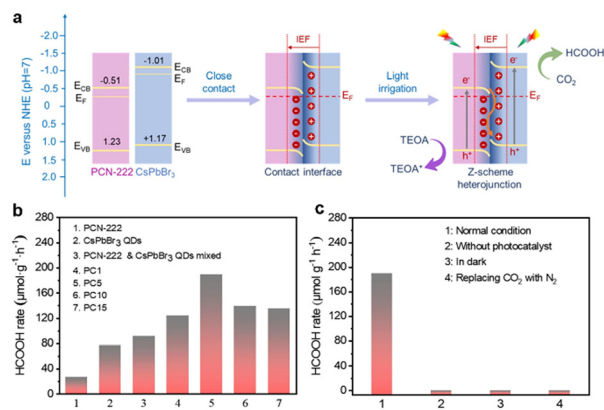

Fig. 19 (a) The proposed scheme of the mechanism of the Z-scheme PCN-222/CsPbBr$_3$ heterojunction under illumination. (b) The performance of photocatalytic reduction of CO_2 over different catalysts. (c) The performance of photocatalytic reduction of CO_2 over PCN-222/CsPbBr$_3$ heterojunction under different conditions.[145] Reproduced with permission. Copyright 2023, Elsevier.
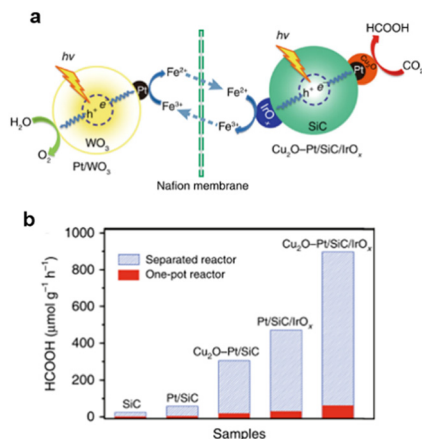
the photoreduction of CO_2 to HCOOH compared to a single part (Fig. 19(b) and (c)) and a 100% selectivity for HCOOH. The efficient charge transfer in the interface between PCN-222 and $CsPbBr_3$ leads to the fabrication of the internal electric field (IEF), which is confirmed by the experimental results as the key to the superior spatial separation of photo-generated electron–hole pairs. Due to the special electron transfer pathway in the Z-scheme heterojunction interface, the outstanding redox ability is achieved for the reduction of CO_2 to HCOOH.

A novel Z-scheme Cu_2O–Pt/SiC/IrO_x catalyst is also constructed and used in an artificial separating oxidation and reduction photocatalytic system for the efficient conversion of CO_2 to HCOOH and the oxidation of H_2O to O_2 (Fig. 20(a)), leading to superior production rates for HCOOH and O_2 of 896.7 (Fig. 20(b)) and 440.7 μmol g^{-1} h^{-1}, respectively, under visible illumination.[131] The specific Z-scheme heterojunction of Cu_2O–Pt/SiC/IrO_x with suitable electronic structure and the separation system lead to long lifetime of photogenerated electron–hole pairs and high selectivity for target production, which are the key reasons for the outstanding performance of reduction of CO_2 and oxidation of H_2O.

Semiconductors and semiconductor heterojunctions, especially Z-type heterojunctions, extend the lifetimes of photogenerated electrons and holes, enhance the redox ability of the catalyst, and then improve the photoreduction performance.

6.2 Heterojunction catalysts for photocatalytic dehydrogenation of HCOOX

Photocatalytic HCOOX dehydrogenation is considered as one of the most promising methods for H_2 generation, because solar energy is clean and abundant.[146,147] Semiconductor photocatalysts are favored by researchers, but there are still some problems such as easy recombination of the photogenerated charge, low energy utilization, and poor catalytic activity.[148] The heterojunction catalyst can achieve efficient photogenerated

charge separation through the design of the interface electronic structure and tune the electron density of the active site to further change the adsorption energy of key intermediate species in the reaction path, so as to improve the above problems.[149] The heterojunction photocatalysts composed of semiconductor and metal-based cocatalysts have been extensively investigated to enhance the activity of solar-driven HCOOX dehydrogenation. And a few semiconductor–semiconductor photocatalyst systems have also been proposed.

6.2.1 Metal–semiconductor heterojunction for photocatalytic dehydrogenation of HCOOX. Noble metals (Pd, Ru, Ir, *etc.*) are widely used as active sites for the dehydrogenation of HCOOX, especially the Pd metal.[76,77,149] The electron structure of Pd NPs is considered as an important factor in improving the performance of dehydrogenation of HCOOX over Pd-based catalysts.[150] The heterojunction constructed from the Pd metal and the semiconductor is an effective approach to tuning the electronic structure of Pd nanoparticles.

Pd nanoparticles (NPs) and g-C_3N_4 (Pd@CN) heterojunction catalysts are successfully designed with a rectifying contact between Pd NPs and g-C_3N_4, which show superior catalytic activity as a photocatalyst under visible light.[150] A typical Mott–Schottky heterojunction forms at the interface of Pd and g-C_3N_4, allowing electrons to flow through the metal–semiconductor interface until Fermi level equilibrium is reached, which causes the conduction band of g-C_3N_4 to bend downward (Fig. 21(a)). The photoluminescence intensity of g-C_3N_4 decreases significantly upon the introduction of Pd NPs, confirming the formation of a heterojunction and the enhanced charge separation at the heterojunction interface. The Mott–Schottky interface separates more electron–hole pairs, and the Schottky barrier prevents electron backflow, facilitating the electron enrichment of Pd-NPs and significantly enhancing the catalytic activity (Fig. 21(b)). More importantly, the enhancement of the catalytic performance of the Mott–Schottky catalyst is related to the wavelength, directly demonstrating the key role of the Mott–Schottky effect in promoting the catalytic activity of Pd@CN.

Alloy metal and semiconductor heterojunction structures can also be designed and developed as excellent photocatalysts for formic acid dehydrogenation.[151] PdAg nanowires (NWs) on graphitic carbon nitride (g-C_3N_4) PdAg@g-C_3N_4 Mott–Schottky heterojunction catalysts offer superior photocatalytic performance of dehydrogenation of formic acid (FA) (TOF = 420 h^{-1}) under visible light at 25 °C.[149] The charge transfer from g-C_3N_4 and Ag to Pd at the heterojunction interface leads to the electron-rich nature of Pd and enhances the catalytic activity and stability of photocatalytic FA dehydrogenation under visible light.

While the high cost and low abundance of the noble metals inhibit their practical application. Therefore, designing an efficient, low-cost, and stable photocatalyst for FA dehydrogenation has attracted much attention. Non-noble metals based on heterojunction catalysts are the potential candidates for the photocatalytic dehydrogenation of formate.[147,148,152] Besides the metals, some metal carbides, nitrides, and phosphides also
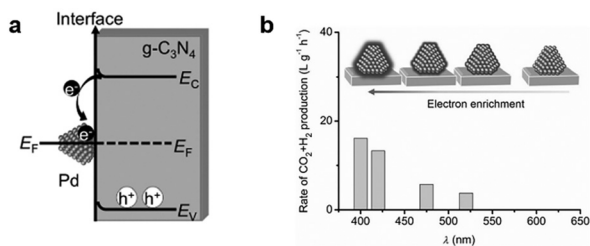
Fig. 21 (a) Scheme for contact interface of the typical Mott–Schottky heterojunction Pd@CN. (b) The activity of photocatalytic dehydrogenation of HCOOH over Pd@CN under the different irradiation wavelengths.[150] Reproduced with permission. Copyright 2013, Wiley VCH.

exhibit metallic properties and can therefore be used to construct metal-based heterojunctions. Among the non-noble metal based catalysts, the corresponding transition-metal phosphides (TMPs) with good conductivity and high chemical stability have been widely investigated in various photocatalytic systems and exhibit superior photocatalytic performances.[147,153–155] All of these properties suggest that TMPs can be ideal cocatalysts for the photocatalytic dehydrogenation of HCOOX.

Iron phosphide (FeP) nanoparticles anchored on CdS nanorods (FeP@CdS) are designed as superior photocatalysts for the dehydrogenation of formic acid, giving an H_2 evolution rate of ~ 556 μmol h^{-1} at pH 3.5 and a high apparent quantum yield of $\sim 54\%$ at 420 nm.[153] The inherent electric field at the interface between FeP and CdS promotes the transfer of outer electrons from CdS to FeP. Due to the fast transfer of electrons from CdS to FeP nanoparticles at the heterojunction interface, photogenerated electron–hole pairs can be rapidly separated, resulting in efficient conversion of solar energy. The FeP co-catalyst also

improves the selectivity of hydrogen production by inhibiting FA dehydration.

A CoP nanoparticle (NP) with a small size is also used as an efficient cocatalyst to construct a CdS/CoP@RGO hybrid for the photocatalytic dehydrogenation of FA (Fig. 22(a)), giving an outstanding production rate of H_2 (182 μmol mg^{-1} h^{-1}) better than the classical Pd/C$_3$N$_4$ photocatalyst (Fig. 22(b)) and robust chemical stability under visible illumination without any additives.[156] CoP plays a vital role in promoting the photo-generated charge separation, leading to the efficient charge transfer in the interface, preferred for the evolution of H_2, which is confirmed by both the DFT and experimental results.

The methods for construction of heterojunctions could be extended to double transition metal-based catalysts. Typical NiCoP nanoparticles anchored to CdS nanorods (NiCoP@CdS NRs) are also synthesized with fast electron transfer from CdS to NiCoP nanoparticles caused by the construction of a heterojunction interface, resulting in the effective separation of electron–hole pairs generated by CdS, which show efficient and robust photocatalytic performance for FA dehydrogenation.[154] The best H_2 evolution and apparent quantum yield (AQY) of photocatalytic HCOOH dehydrogenation are 354 μmol mg^{-1} h^{-1} with 100% selectivity and 45.5%, respectively, under the optimal conditions at 420 nm. Furthermore, the H_2 evolution rate can be maintained after a longtime test of 48 h under visible illumination and optimal conditions.

The nitrides of transition metals with metallic properties can also be used as cocatalysts to construct metal–semiconductor heterojunctions for the photocatalytic dehydrogenation of formate. A specific CdS/W$_2$N$_3$ heterojunction photocatalyst system is synthesized for efficient photo-decomposition of HCOOH to achieve the
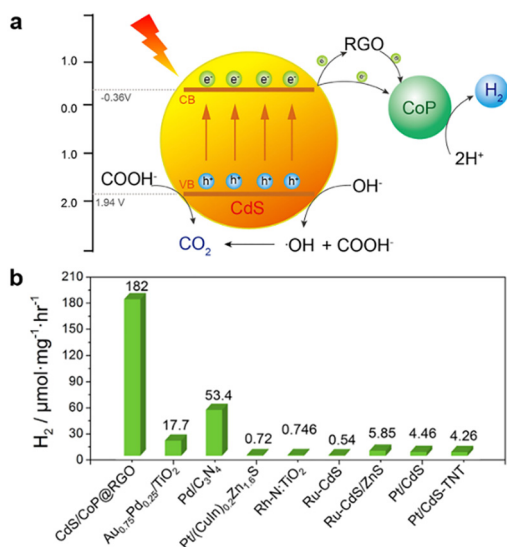
Fig. 22 (a) The schematic of the proposed process for the dehydrogenation of HCOOH over a CdS/CoP@RGO sample under illumination. (b) The H_2 evolution rate for the dehydrogenation of HCOOH over different catalysts under illumination.[156] Reproduced with permission. Copyright 2018, Elsevier.
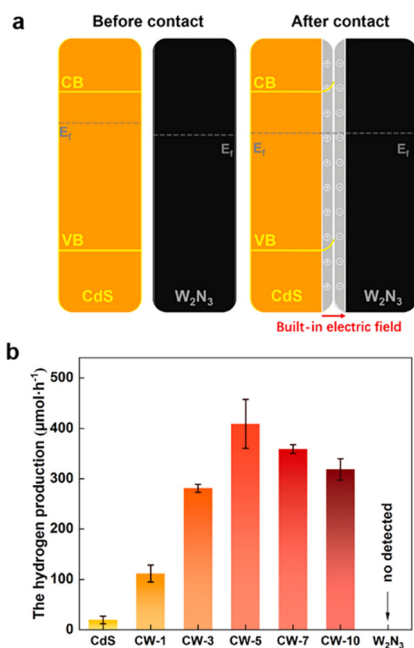
Fig. 23 (a) The scheme of the heterojunction constructed from W$_2$N$_3$ and CdS. (b) H_2 evolution rate over different samples in 1.0 M HCOOH solution.[157] Reproduced with permission. Copyright 2023, Elsevier.

products from H_2 to syngas with tunable selectivity under sunlight.[157] Due to the difference in the work function of W_2N_3 and CdS, electrons can be transferred from CdS with a higher Fermi level to W_2N_3 with a lower Fermi level in the contact interface, forming a strong interaction (Fig. 23(a)), which improves the separation of photogenerated carriers. The W_2N_3 cocatalyst as reduction active sites in the CdS/W_2N_3 heterojunction can achieve a remarkable H_2 production rate of 408.90 μmol h^{-1} in the photocatalytic reaction (Fig. 23(b)).

The heterojunction structure of metal co-catalysts and photo-semiconductors improves the efficiency of photoelectrons and regulates the electronic structure of the metal surface, which can greatly improve the performance of photocatalytic HCOOX dehydrogenation. In addition to noble metals, non-noble metals, metal phosphides, and nitrides can be used for constructing efficient heterojunction catalysts as co-catalysts with suitable photo-semiconductors, which have the potential for practical application.

6.2.2 Semiconductor–semiconductor heterojunctions for photocatalytic dehydrogenation of HCOOX. The high redox ability of the Z-scheme heterojunction is the most remarkable of the different types of semiconductor–semiconductor heterojunctions.[46] A more positive hole potential and efficient charge separation can be achieved by constructing the Z-scheme with suitable semiconductors, which are favorable for the photocatalytic dehydrogenation of HCOOX.

Graphitic carbon nitride (g-CN) as a typical semiconductor is widely used for photocatalytic reactions, because of the suitable band structure and cost.[158] A novel Z-scheme heterojunction g-

CN/Ag/Ag_3PO_4–AgPd photocatalyst is synthesized by choosing a secondary semiconductor of Ag_3PO_4 with a more positive potential of valence band than g-CN for FA dehydrogenation, giving a superior turnover frequency (TOF) of 2107 h^{-1} at 50 °C under white-LED illumination (Fig. 24(b)). The typically designed g-CN/Ag/Ag_3PO_4–AgPd photocatalysts with specific interfaces highly boost the photocatalytic dehydrogenation of HCOOH by providing a more positive potential of the hole and promoting the charge separation efficiency of the heterojunction catalyst (Fig. 24(a)).

Compared with the widespread application of metal–semiconductor heterojunctions in photocatalytic dehydrogenation, semiconductor–semiconductor heterojunctions have been studied relatively little. A Z-scheme heterojunction as a typical semiconductor–semiconductor heterojunction structure can efficiently separate photogenerated charges and improve the oxidation capacity of photogenerated holes, which is conducive to the photocatalytic formate dehydrogenation reaction. Therefore, the rational design of a Z-type heterojunction to achieve efficient photocatalytic HCOOX dehydrogenation is still a worthy research direction.

7. Conclusions

The interconversion between CO_2/HCO_3^- and HCOOX is an efficient way to chemically reuse excess CO_2 and achieve the goal of safe storage and transportation of hydrogen energy. To realize the actual use of the interconversion circle, developing efficient and sustainable heterogeneous catalysts is always of the top priority. Heterojunction catalysts, including metal–semiconductor heterojunctions and semiconductor–semiconductor heterojunctions, have been investigated to change the electronic structure of the active site and specifically regulate the activity, selectivity, and stability of the catalysts. In this review, the effects of interfacial electronic structures in different heterojunctions for the CO_2/HCO_3^- and HCOOH/HCOO$^-$ interconversion driven by different energy forms are described in detail, and the potential practical use of heterojunction catalysts in various energy forms is proposed.

In the thermal catalysis system, the heterojunction catalysts composed of noble metal-based active centres highly elevate the activity and atomic utilization of noble metals. The electronic interface in the heterojunction catalyst regulates the electron density of the metal, reduces the size of the nanoparticles of the noble metal, and enhances the activation of the reactants, leading to the efficient performance of hydrogenation and dehydrogenation reactions. According to the best existing heterojunction catalysts, it takes hours to achieve usable kilogram level hydrogen storage, and the release of 1 kg of hydrogen can be controlled within 40 minutes. As a result, the heterojunction type catalysts have shown the potential to achieve kilogram-scale reactions of H_2 storage and release for practical applications, while the development of cheaper and more efficient non-noble metal heterojunction catalysts remains the key to expanding their use at relatively low cost.

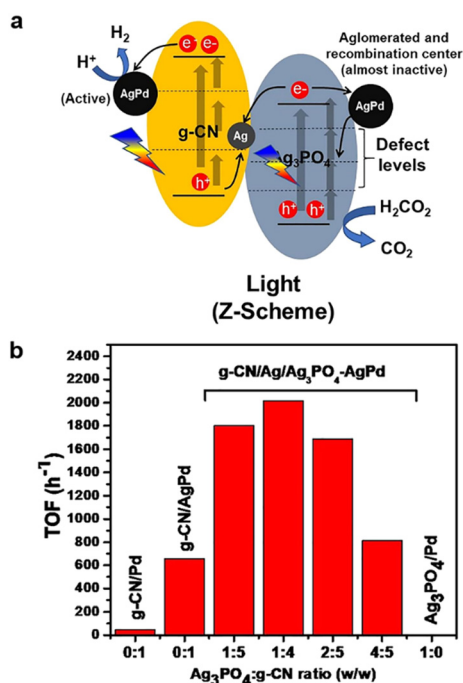Fig. 24 (a) The scheme of HCOOH dehydrogenation reaction over g-CN/Ag/Ag_3PO_4–AgPd under illumination. (b) The turnover frequency (TOF) values of different catalysts at 50 °C under visible light.[158] Reproduced with permission. Copyright 2021, Elsevier.

In the electrocatalytic system, non-noble metal Sn, Bi, and In-based heterojunction materials have shown great prospects for achieving efficient CO_2 hydrogenation performance. The interfacial electron regulations of heterojunction catalysts based on cheap metal elements also accelerate electron transport, enhance the activation of CO_2, and thus promote the final activity and selectivity. At present, the reaction rate of electrochemical hydrogenation of CO_2 to formate over the optimal catalyst is still at the millimolar level under industrial current (>200 mA cm^{-2}), and there is still a big gap from achieving the usable hydrogen storage capacity of 1 kg. In order to achieve more valuable electrocatalytic hydrogenation, in addition to the design of better heterojunction catalysts, large-area electrodes and appropriate reactors are also the future directions. The electrocatalytic dehydrogenation of formic acid to release hydrogen is rarely reported, because of the very few usage scenarios. Electrooxidation of formic acid remains the mainstream to release energy for formic acid fuel cells.

In the photocatalytic system, heterojunction catalysts with the rectifying contact improve the separation of photogenerated charge and the redox ability of the catalyst for the efficient photo-driven interconversion of CO_2/HCO_3^- and HCOOX, which shows an attractive prospect for the practical application. However, the hydrogenation rate and hydrogen evolution rate that are based on the interconversion of CO_2/HCO_3^- and HCOOX over the state-of-art photocatalysts are still limited at the micromolar level, far apart from practical uses in the kilogram-scale hydrogen storage.

The exploration and application of reusable catalysts in the CO_2–HCOOX interconversion reaction is still in its infancy. Heterojunction-based catalysts composed of non-noble metals promise great potential in largely boosting the intrinsic activity for interconversion of CO_2/HCO_3^- and HCOOX. In general, studies on developing powerful catalysts and designing reactors with good control of the energy input and gas diffusion to boost the multiphase reactions are still highly required to meet the requirements of large-scale applications.

Author contributions

X.-H. L. and Y.-S. X. conceived the project and co-wrote the original manuscript. D. X. helped to collect documents and organize images. J.-S. C. and X.-H. L. oversaw all of the phases and revised the manuscript. All of the authors discussed the experimental results and commented on the manuscript.

Conflicts of interest

There are no conflicts to declare.

Acknowledgements

Notes and references

1 Y. X. Liu, H. H. Wang, T. J. Zhao, B. Zhang, H. Su, Z. H. Xue, X. H. Li and J. S. Chen, Schottky barrier induced coupled interface of electron-rich N-doped carbon and electron-deficient Cu: in-built Lewis acid-base pairs for highly efficient CO_2 fixation, *J. Am. Chem. Soc.*, 2019, **141**, 38–41.

2 I. Sullivan, A. Goryachev, I. A. Digdaya, X. Li, H. A. Atwater, D. A. Vermaas and C. Xiang, Coupling electrochemical CO_2 conversion with CO_2 capture, *Nat. Catal.*, 2021, **4**, 952–958.

3 X. Chang, T. Wang and J. Gong, CO_2 photo-reduction: insights into CO_2 activation and reaction on surfaces of photocatalysts, *Energy Environ. Sci.*, 2016, **9**, 2177–2196.

4 Y. Jiang, Y. Sung, C. Choi, G. Joo Bang, S. Hong, X. Tan, T. S. Wu, Y. L. Soo, P. Xiong and M. Meng Jung LI, Single-atom molybdenum-N_3 sites for selective hydrogenation of CO_2 to CO, *Angew. Chem., Int. Ed.*, 2022, **61**, e202203836.

5 Y. S. Ham, S. Choe, M. J. Kim, T. Lim, S. K. Kim and J. J. Kim, Electrodeposited Ag catalysts for the electrochemical reduction of CO_2 to CO, *Appl. Catal., B*, 2017, **208**, 35–43.

6 L. Han, S. Song, M. Liu, S. Yao, Z. Liang, H. Cheng, Z. Ren, W. Liu, R. Lin and G. Qi, Stable and efficient single-atom Zn catalyst for CO_2 reduction to CH_4, *J. Am. Chem. Soc.*, 2020, **142**, 12563–12567.

7 D. Xiao, X. Bao, M. Zhang, Z. Li, Z. Wang, Y. Gao, Z. Zheng, P. Wang, H. Cheng and Y. Liu, Stabilizing Cu_2O for enhancing selectivity of CO_2 electroreduction to C_2H_4 with the modification of Pd nanoparticles, *Chem. Eng. J.*, 2023, **452**, 139358.

8 B. Yang, W. Deng, L. Guo and T. Ishihara, Copper-ceria solid solution with improved catalytic activity for hydrogenation of CO_2 to CH_3OH, *Chin. J. Catal.*, 2020, **41**, 1348–1359.

9 H. Song, N. Zhang, C. Zhong, Z. Liu, M. Xiao and H. Gai, Hydrogenation of CO_2 into formic acid using a palladium catalyst on chitin, *New J. Chem.*, 2017, **41**, 9170–9177.

10 G. Wen, B. Ren, X. Wang, D. Luo, H. Dou, Y. Zheng, R. Gao, J. Gostick, A. Yu and Z. Chen, Continuous CO_2 electrolysis using a CO_2 exsolution-induced flow cell, *Nat. Energy*, 2022, **7**, 978–988.

11 S. Fang, M. Rahaman, J. Bharti, E. Reisner, M. Robert, G. A. Ozin and Y. H. Hu, Photocatalytic CO_2 reduction, *Nat. Rev. Methods Primers*, 2023, **3**, 61.

12 Y. C. Tan, K. B. Lee, H. Song and J. Oh, Modulating local CO_2 concentration as a general strategy for enhancing C–C coupling in CO_2 electroreduction, *Joule*, 2020, **4**, 1104–1120.

13 X. Wang, Y. Wang, M. Gao, J. Shen, X. Pu, Z. Zhang, H. Lin and X. Wang, $BiVO_4/Bi_4Ti_3O_{12}$ heterojunction enabling efficient photocatalytic reduction of CO_2 with H_2O to CH_3OH and CO, *Appl. Catal., B*, 2020, **270**, 118876.

14 W. Jiao, Y. Xie, F. He, K. Wang, Y. Ling, Y. Hu, J. Wang, H. Ye, J. Wu and Y. Hou, A visible light-response flower-like La-doped BiOBr nanosheets with enhanced performance for photoreducing CO_2 to CH_3OH, *Chem. Eng. J.*, 2021, **418**, 129286.

15 P. Li, L. Liu, W. An, H. Wang, H. Guo, Y. Liang and W. Cui, Ultrathin porous g-C_3N_4 nanosheets modified with AuCu alloy nanoparticles and C–C coupling photothermal catalytic reduction of CO_2 to ethanol, *Appl. Catal., B*, 2020, **266**, 118618.

16 H. Zhang, C. Zhu, R. Liu, Q. Fang, S. Song and Y. Shen, Insight into the island-sea effect of Cu–N–C for enhanced CO_2 eletroreduction selectively towards C_2H_4, *Appl. Catal., B*, 2024, **343**, 123566.

17 W. J. Dong, I. A. Navid, Y. Xiao, T. H. Lee, J. W. Lim, D. Lee, H. W. Jang, J.-L. Lee and Z. Mi, Bi catalysts supported on GaN nanowires toward efficient photoelectrochemical CO_2 reduction, *J. Mater. Chem. A*, 2022, **10**, 7869–7877.

18 J. Wang, X. Zheng, G. Wang, Y. Cao, W. Ding, J. Zhang, H. Wu, J. Ding, H. Hu and X. Han, Defective bimetallic selenides for selective CO_2 electroreduction to CO, *Adv. Mater.*, 2022, **34**, 2106354.

19 A. Behr and K. Nowakowski, *Adv. Inorg. Chem.*, Elsevier, 2014, vol. 66, pp. 223–258.

20 H. Park, J. Choi, H. Kim, E. Hwang, D. Ha, S. H. Ahn and S. Kim, AgIn dendrite catalysts for electrochemical reduction of CO_2 to CO, *Appl. Catal., B*, 2017, **219**, 123–131.

21 Z. Ding, Y. Xu, Q. Yang and R. Hou, Pd-modified CuO–ZnO–ZrO_2 catalysts for CH_3OH synthesis from CO_2 hydrogenation, *Int. J. Hydrogen Energy*, 2022, **47**, 24750–24760.

22 M. S. Maru, S. Ram, J. H. Adwani and R. S. Shukla, Selective and direct hydrogenation of CO_2 for the synthesis of formic acid over a rhodium hydrotalcite (Rh-HT) catalyst, *ChemistrySelect*, 2017, **2**, 3823–3830.

23 W. H. Wang, Y. Himeda, J. T. Muckerman, G. F. Manbeck and E. Fujita, CO_2 hydrogenation to formate and methanol as an alternative to photo-and electrochemical CO_2 reduction, *Chem. Rev.*, 2015, **115**, 12936–12973.

24 S. Jiang, X. Liu, S. Zhai, X. Ci, T. Yu, L. Sun, D. Zhai, W. Deng and G. Ren, Additive-free CO_2 hydrogenation to pure formic acid solution via amine-modified Pd catalyst at room temperature, *Green Chem.*, 2023, **25**, 6025–6031.

25 W. J. Dong, I. A. Navid, Y. Xiao, J. W. Lim, J. L. Lee and Z. Mi, CuS-decorated GaN nanowires on silicon photocathodes for converting CO_2 mixture gas to HCOOH, *J. Am. Chem. Soc.*, 2021, **143**, 10099–10107.

26 Y. X. Duan, K. H. Liu, Q. Zhang, J. M. Yan and Q. Jiang, Efficient CO_2 reduction to HCOOH with high selectivity and energy efficiency over Bi/rGO catalyst, *Small Methods*, 2020, **4**, 1900846.

27 L. Zou, Q. Liu, Q. Zhang, Z. Zhu, Y. Huang and Z. Liang, Synthesis of bimetallic Pd-Based/activated carbon catalyst by biomass-reduction method for highly efficient hydrogen storage system based on CO_2/formate, *Ind. Eng. Chem. Res.*, 2022, **61**, 2455–2468.

28 A. Boddien, C. Federsel, P. Sponholz, D. Mellmann, R. Jackstell, H. Junge, G. Laurenczy and M. Beller, Towards

29 W. Yan, J. Zhang, S. Lu and Y. Xiang, Tuning dehydrogenation behavior of formic acid on boosting cell performance of formic acid fuel cell at elevated temperatures, *J. Power Sources*, 2022, **544**, 231877.

30 R. Bhaskaran, B. G. Abraham and R. Chetty, Recent advances in electrocatalysts, mechanism, and cell architecture for direct formic acid fuel cells, *Wiley Interdiscip. Rev.: Energy Environ.*, 2022, **11**, e419.

31 S. Uhm, H. J. Lee and J. Lee, Understanding underlying processes in formic acid fuel cells, *Phys. Chem. Chem. Phys.*, 2009, **11**, 9326–9336.

32 S. Moret, P. J. Dyson and G. Laurenczy, Direct synthesis of formic acid from carbon dioxide by hydrogenation in acidic media, *Nat. Commun.*, 2014, **5**, 4017.

33 C. Fellay, P. J. Dyson and G. Laurenczy, A viable hydrogen-storage system based on selective formic acid decomposition with a ruthenium catalyst, *Angew. Chem., Int. Ed.*, 2008, **47**, 3966–3968.

34 H. Park, J. H. Lee, E. H. Kim, K. Y. Kim, Y. H. Choi, D. H. Youn and J. S. Lee, A highly active and stable palladium catalyst on a g-C_3N_4 support for direct formic acid synthesis under neutral conditions, *Chem. Commun.*, 2016, **52**, 14302–14305.

35 Z. Wang, C. Wang, S. Mao, Y. Gong, Y. Chen and Y. Wang, Pd nanoparticles anchored on amino-functionalized hierarchically porous carbon for efficient dehydrogenation of formic acid under ambient conditions, *J. Mater. Chem. A*, 2019, **7**, 25791–25795.

36 W. Leitner, E. Dinjus and F. Gaßner, Activation of carbon dioxide: IV. Rhodium-catalysed hydrogenation of carbon dioxide to formic acid, *J. Organomet. Chem.*, 1994, **475**, 257–266.

37 A. Boddien, F. Gärtner, C. Federsel, P. Sponholz, D. Mellmann, R. Jackstell, H. Junge and M. Beller, CO_2-"Neutral" hydrogen storage based on bicarbonates and formates, *Angew. Chem., Int. Ed.*, 2011, **50**, 6411–6414.

38 R. Sun, Y. Liao, S. T. Bai, M. Zheng, C. Zhou, T. Zhang and B. F. Sels, Heterogeneous catalysts for CO_2 hydrogenation to formic acid/formate: from nanoscale to single atom, *Energy Environ. Sci. Technol.*, 2021, **14**, 1247–1285.

39 N. Onishi, R. Kanega, H. Kawanami and Y. Himeda, Recent progress in homogeneous catalytic dehydrogenation of formic acid, *Molecules*, 2022, **27**, 455.

40 Z. Fang and W. Chen, Recent advances in formic acid electro-oxidation: From the fundamental mechanism to electrocatalysts, *Nanoscale Adv.*, 2021, **3**, 94–105.

41 P. Verma, S. Zhang, S. Song, K. Mori, Y. Kuwahara, M. Wen, H. Yamashita and T. An, Recent strategies for enhancing the catalytic activity of CO_2 hydrogenation to formate/formic acid over Pd-based catalyst, *J. CO2 Util.*, 2021, **54**, 101765.

42 A. Álvarez, A. Bansode, A. Urakawa, A. V. Bavykina, T. A. Wezendonk, M. Makkee, J. Gascon and F. Kapteijn, Challenges in the greener production of formates/formic

the development of a hydrogen battery, *Energy Environ. Sci.*, 2012, **5**, 8907–8911.

acid, methanol, and DME by heterogeneously catalyzed CO_2 hydrogenation processes, *Chem. Rev.*, 2017, **117**, 9804–9838.

43 X. Jiang, X. Nie, X. Guo, C. Song and J. Chen, Recent advances in carbon dioxide hydrogenation to methanol via heterogeneous catalysis, *Chem. Rev.*, 2020, **120**, 7984–8034.

44 X. Li, M. Baar, S. Blechert and M. Antonietti, Facilitating room-temperature Suzuki coupling reaction with light: Mott–Schottky photocatalyst for C–C coupling, *Sci. Rep.*, 2013, **3**, 1743.

45 X. Lin, S. Zhang, D. Xu, J. Zhang, Y. Lin, G. Zhai, H. Su, Z. Xue, X. Liu and M. Antonietti, Electrochemical activation of C–H by electron-deficient W_2C nanocrystals for simultaneous alkoxylation and hydrogen evolution, *Nat. Commun.*, 2021, **12**, 3882.

46 P. Zhou, J. Yu and M. Jaroniec, All-solid-state Z-scheme photocatalytic systems, *Adv. Mater.*, 2014, **26**, 4920–4935.

47 J. Yao, M. Zhang, X. Ma, L. Xu, F. Gao, J. Xiao and H. Gao, Interfacial electronic modulation of CoP–CoO p–p type heterojunction for enhancing oxygen evolution reaction, *J. Colloid Interface Sci.*, 2022, **607**, 1343–1352.

48 T. Ioannides and X. Verykios, Charge transfer in metal catalysts supported on doped TiO_2: a theoretical approach based on metal–semiconductor contact theory, *J. Catal.*, 1996, **161**, 560–569.

49 X.-H. Li and M. Antonietti, Metal nanoparticles at mesoporous N-doped carbons and carbon nitrides: functional Mott–Schottky heterojunctions for catalysis, *Chem. Soc. Rev.*, 2013, **42**, 6593–6604.

50 G. Zhang, Z. Wang and J. Wu, Construction of a Z-scheme heterojunction for high-efficiency visible-light-driven photocatalytic CO_2 reduction, *Nanoscale*, 2021, **13**, 4359–4389.

51 D. Xu, S. N. Zhang, J. S. Chen and X. H. Li, Design of the synergistic rectifying interfaces in Mott–Schottky catalysts, *Chem. Rev.*, 2022, **123**, 1–30.

52 Z. Zhang and J. T. Yates Jr, Band bending in semiconductors: chemical and physical consequences at surfaces and interfaces, *Chem. Rev.*, 2012, **112**, 5520–5551.

53 Y. X. Lin, S. N. Zhang, Z. H. Xue, J. J. Zhang, H. Su, T. J. Zhao, G. Y. Zhai, X. H. Li, M. Antonietti and J. S. Chen, Boosting selective nitrogen reduction to ammonia on electron-deficient copper nanoparticles, *Nat. Commun.*, 2019, **10**, 4380.

54 N. Tian, H. Huang, C. Liu, F. Dong, T. Zhang, X. Du, S. Yu and Y. Zhang, In situ co-pyrolysis fabrication of CeO_2/g-C_3N_4 n–n type heterojunction for synchronously promoting photo-induced oxidation and reduction properties, *J. Mater. Chem. A*, 2015, **3**, 17120–17129.

55 K. He, T. Tadesse Tsega, X. Liu, J. Zai, X. H. Li, X. Liu, W. Li, N. Ali and X. Qian, Utilizing the space-charge region of the FeNi-LDH/CoP p–n junction to promote performance in oxygen evolution electrocatalysis, *Angew. Chem., Int. Ed.*, 2019, **58**, 11903–11909.

56 L. H. Sun, Q. Y. Li, S. N. Zhang, D. Xu, Z. H. Xue, H. Su, X. Lin, G. Y. Zhai, P. Gao and S. I. Hirano, Heterojunction-based electron donors to stabilize and activate ultrafine Pt nanoparticles for efficient hydrogen atom dissociation and gas evolution, *Angew. Chem., Int. Ed.*, 2021, **60**, 25766–25770.

57 D. Xu, X. Lin, Q. Y. Li, S. N. Zhang, S. Y. Xia, G. Y. Zhai, J. S. Chen and X. H. Li, Boosting mass exchange between Pd/NC and MoC/NC dual junctions via electron exchange for cascade CO_2 fixation, *J. Am. Chem. Soc.*, 2022, **144**, 5418–5423.

58 S. Y. Xia, Q. Y. Li, S. N. Zhang, D. Xu, X. Lin, L. H. Sun, J. Xu, J. S. Chen, G. D. Li and X. H. Li, Size-dependent electronic interface effect of Pd nanocube-based heterojunctions on universally boosting phenol hydrogenation reactions, *Chin. J. Catal.*, 2023, **49**, 180–187.

59 L. H. Sun, Q. Y. Li, Y. S. Xu, S. Y. Xia, D. Xu, X. Lin, J. Xu, J. S. Chen, G. D. Li and X. H. Li, Tunable hydrogen coverage on electron-deficient platinum nanoparticles for efficient hydrogenation reactions, *Nano Res.*, 2023, **16**, 8751–8756.

60 X. H. Li, M. Baar, S. Blechert and M. Antonietti, Facilitating room-temperature Suzuki coupling reaction with light: Mott–Schottky photocatalyst for C–C-coupling, *Sci. Rep.*, 2013, **3**, 1743.

61 S. N. Zhang, P. Gao, L. H. Sun, J. S. Chen and X. H. Li, Tunable surface electric field of electrocatalysts via constructing Schottky heterojunctions for selective conversion of trash ions to treasures, *Chem. – Eur. J.*, 2022, **28**, e202103918.

62 Z. H. Xue, S. N. Zhang, Y. X. Lin, H. Su, G. Y. Zhai, J. T. Han, Q. Y. Yu, X. H. Li, M. Antonietti and J. S. Chen, Electrochemical reduction of N_2 into NH_3 by donor-acceptor couples of Ni and Au nanoparticles with a 67.8% faradaic efficiency, *J. Am. Chem. Soc.*, 2019, **141**, 14976–14980.

63 P. G. Jessop, T. Ikariya and R. Noyori, Homogeneous hydrogenation of carbon dioxide, *Chem. Rev.*, 1995, **95**, 259–272.

64 X. Zhang, A. Li, H. Tang, Y. Xu, X. Qin, Z. Jiang, Q. Yu, W. Zhou, L. Chen and M. Wang, Carbonate hydrogenated to formate in the aqueous phase over nickel/TiO_2 catalysts, *Angew. Chem., Int. Ed.*, 2023, **62**, e202307061.

65 M. S. Jeletic, M. T. Mock, A. M. Appel and J. C. Linehan, A cobalt-based catalyst for the hydrogenation of CO_2 under ambient conditions, *J. Am. Chem. Soc.*, 2013, **135**, 11533–11536.

66 S. Jiang, J. Sun, S. Zhai, T. Yu, L. Sun, L. Yang, D. Zhai, C. Liu, Z. Li and G. Ren, Ambient CO_2 capture and conversion into liquid fuel and fertilizer catalyzed by a PdAu nano-alloy, *Cell Rep. Phys. Sci.*, 2023, **4**, 101248.

67 O. Y. Gutiérrez, K. Grubel, J. Kothandaraman, J. A. Lopez Ruiz, K. P. Brooks, M. E. Bowden and T. Autrey, Using earth abundant materials for long duration energy storage: electro-chemical and thermo-chemical cycling of bicarbonate/formate, *Green Chem.*, 2023, **25**, 4222–4233.

68 J. Su, M. Lu and H. Lin, High yield production of formate by hydrogenating CO_2 derived ammonium carbamate/

carbonate at room temperature, *Green Chem.*, 2015, **17**, 2769–2773.

69 N. Yodsin, C. Rungnim, S. Tungkamani, V. Promarak, S. Namuangruk and S. Jungsuttiwong, DFT study of catalytic CO_2 hydrogenation over Pt-decorated carbon nanocones: H_2 dissociation combined with the spillover mechanism, *J. Phys. Chem. C*, 2019, **124**, 1941–1949.

70 T. Ren, Z. Miao, L. Ren, H. Xie, Q. Li and C. Xia, Nanostructure engineering of Sn-based catalysts for efficient electrochemical CO_2 reduction, *Small*, 2023, **19**, 2205168.

71 W. Ju, F. Jiang, H. Ma, Z. Pan, Y. B. Zhao, F. Pagani, D. Rentsch, J. Wang and C. Battaglia, Electrocatalytic reduction of gaseous CO_2 to CO on Sn/Cu-nanofiber-based gas diffusion electrodes, *Adv. Energy Mater.*, 2019, **9**, 1901514.

72 Y. Zhang, F. Li, J. Dong, K. Jia, T. Sun and L. Xu, Recent advances in designing efficient electrocatalysts for electrochemical carbon dioxide reduction to formic acid/formate, *J. Electroanal. Chem.*, 2023, **928**, 117018.

73 X. An, S. Li, A. Yoshida, T. Yu, Z. Wang, X. Hao, A. Abudula and G. Guan, Bi-doped SnO nanosheets supported on Cu foam for electrochemical reduction of CO_2 to HCOOH, *ACS Appl. Mater. Interfaces*, 2019, **11**, 42114–42122.

74 X. Yang, P. Deng, D. Liu, S. Zhao, D. Li, H. Wu, Y. Ma, B. Y. Xia, M. Li and C. Xiao, Partial sulfuration-induced defect and interface tailoring on bismuth oxide for promoting electrocatalytic CO_2 reduction, *J. Mater. Chem. A*, 2020, **8**, 2472–2480.

75 F. Yang, C. Jiang, M. Ma, F. Shu, X. Mao, W. Yu, J. Wang, Z. Zeng and S. Deng, Solid-state synthesis of Cu nanoparticles embedded in carbon substrate for efficient electrochemical reduction of carbon dioxide to formic acid, *Chem. Eng. J.*, 2020, **400**, 125879.

76 Y. X. Luo, W. Nie, Y. Ding, Q. Yao, G. Feng and Z. Lu, Robust hydrogen production from additive-free formic acid via mesoporous silica-confined Pd–ZrO₂ nanoparticles at room temperature, *ACS Appl. Energy Mater.*, 2021, **4**, 4945–4954.

77 N. Nouruzi, M. Dinari, N. Mokhtari, M. Farajzadeh, B. Gholipour and S. Rostamnia, Selective catalytic generation of hydrogen over covalent organic polymer supported Pd nanoparticles (COP-Pd), *Mol. Catal.*, 2020, **493**, 111057.

78 X. Gu, Z. Lu, H. Jiang, T. Akita and Q. Xu, Synergistic catalysis of metal-organic framework-immobilized Au–Pd nanoparticles in dehydrogenation of formic acid for chemical hydrogen storage, *J. Am. Chem. Soc.*, 2011, **133**, 11822–11825.

79 X. Liu, T. Jacob and W. Gao, Progress of fundamental mechanism of formic acid decomposition and electrooxidation, *J. Energy Chem.*, 2022, **70**, 292–309.

80 F. Z. Song, Q. L. Zhu, X. Yang, W. W. Zhan, P. Pachfule, N. Tsumori and Q. Xu, Metal–organic framework templated porous carbon-metal oxide/reduced graphene oxide as superior support of bimetallic nanoparticles for efficient hydrogen generation from formic acid, *Adv. Energy Mater.*, 2018, **8**, 1701416.

81 M. Liang, T. Xia, H. Gao, K. Zhao, T. Cao, M. Deng, X. Ren, S. Li, H. Guo and R. Wang, Modulating reaction pathways of formic acid oxidation for optimized electrocatalytic performance of PtAu/CoNC, *Nano Res.*, 2022, **15**, 1221–1229.

82 A. Ferre Vilaplana, J. V. Perales Rondón, C. Buso Rogero, J. M. Feliu and E. Herrero, Formic acid oxidation on platinum electrodes: a detailed mechanism supported by experiments and calculations on well-defined surfaces, *J. Mater. Chem. A*, 2017, **5**, 21773–21784.

83 W. Chen, A. Yu, Z. Sun, B. Zhu, J. Cai and Y. Chen, Probing complex eletrocatalytic reactions using electrochemical infrared spectroscopy, *Curr. Opin. Electrochem.*, 2019, **14**, 113–123.

84 K. Nakajima, M. Tominaga, M. Waseda, H. Miura and T. Shishido, Highly efficient supported palladium-gold alloy catalysts for hydrogen storage based on ammonium bicarbonate/formate redox cycle, *ACS Sustainable Chem. Eng.*, 2019, **7**, 6522–6530.

85 Z. Chen, C. A. M. Stein, R. Qu, N. Rockstroh, S. Bartling, J. Weiß, C. Kubis, K. Junge, H. Junge and M. Beller, Designing a robust palladium catalyst for formic acid dehydrogenation, *ACS Catal.*, 2023, **13**, 4835–4841.

86 M. Calabrese, D. Russo, A. di Benedetto, R. Marotta and R. Andreozzi, Formate/bicarbonate interconversion for safe hydrogen storage: a review, *Renewable Sustainable Energy Rev.*, 2023, **173**, 113102.

87 Z. Wang, J. Qian, Z. Sun, Z. Zhang, M. He and Q. Chen, Application of heterogeneous catalysis in formic acid-based hydrogen cycle system, *Catalysts*, 2023, **13**, 1168.

88 J. Su, L. Yang, M. Lu and H. Lin, Highly efficient hydrogen storage system based on ammonium bicarbonate/formate redox equilibrium over palladium nanocatalysts, *ChemSusChem*, 2015, **8**, 813–816.

89 Y. Kim and D. H. Kim, Hydrogen production from formic acid dehydrogenation over a Pd supported on N-doped mesoporous carbon catalyst: a role of nitrogen dopant, *Appl. Catal., A*, 2020, **608**, 117887.

90 Z. Zhang, L. Zhang, S. Yao, X. Song, W. Huang, M. J. Hülsey and N. Yan, Support-dependent rate-determining step of CO_2 hydrogenation to formic acid on metal oxide supported Pd catalysts, *J. Catal.*, 2019, **376**, 57–67.

91 M. D. Fernández Martínez and C. Godard, Hydrogenation of CO_2 into formates by ligand-capped palladium heterogeneous catalysts, *ChemCatChem*, 2023, **15**, e202201408.

92 K. Mori, T. Sano, H. Kobayashi and H. Yamashita, Surface engineering of a supported PdAg catalyst for hydrogenation of CO_2 to formic acid: elucidating the active Pd atoms in alloy nanoparticles, *J. Am. Chem. Soc.*, 2018, **140**, 8902–8909.

93 G. Yang, Y. Kuwahara, K. Mori, C. Louis and H. Yamashita, PdAg alloy nanoparticles encapsulated in N-doped microporous hollow carbon spheres for hydrogenation of CO_2 to formate, *Appl. Catal., B*, 2021, **283**, 119628.

94 Q. Liu, X. Yang, L. Li, S. Miao, Y. Li, Y. Li, X. Wang, Y. Huang and T. Zhang, Direct catalytic hydrogenation of

CO_2 to formate over a Schiff-base-mediated gold nanocatalyst, *Nat. Commun.*, 2017, **8**, 1407.

95 K. Christmann, Interaction of hydrogen with solid surfaces, *Surf. Sci. Rep.*, 1988, **9**, 1–163.

96 C. Mondelli, B. Puértolas, M. Ackermann, Z. Chen and J. Pérez Ramírez, Enhanced base-free formic acid production from CO_2 on Pd/g-C_3N_4 by tuning of the carrier defects, *ChemSusChem*, 2018, **11**, 2859–2869.

97 C. J. Stalder, S. Chao, D. P. Summers and M. S. Wrighton, Supported palladium catalysts for the reduction of sodium bicarbonate to sodium formate in aqueous solution at room temperature and one atmosphere of hydrogen, *J. Am. Chem. Soc.*, 1983, **105**, 6318–6320.

98 E. González, C. Marchant, C. Sepúlveda, R. García, I. T. Ghampson, N. Escalona and J. L. García Fierro, Hydrogenation of sodium hydrogen carbonate in aqueous phase using metal/activated carbon catalysts, *Appl. Catal., B*, 2018, **224**, 368–375.

99 Q. Y. Bi, J. D. Lin, Y. M. Liu, X. L. Du, J. Q. Wang, H. Y. He and Y. Cao, An aqueous rechargeable formate-based hydrogen battery driven by heterogeneous Pd catalysis, *Angew. Chem., Int. Ed.*, 2014, **53**, 13583–13587.

100 F. Wang, J. Xu, X. Shao, X. Su, Y. Huang and T. Zhang, Palladium on nitrogen-doped mesoporous carbon: a bifunctional catalyst for formate-based, carbon-neutral hydrogen storage, *ChemSusChem*, 2016, **9**, 246–251.

101 S. Masuda, K. Mori, Y. Kuwahara, C. Louis and H. Yamashita, Additive-free aqueous phase synthesis of formic acid by direct CO_2 hydrogenation over a PdAg catalyst on a hydrophilic n-doped polymer-silica composite support with high CO_2 affinity, *ACS Appl. Energy Mater.*, 2020, **3**, 5847–5855.

102 Z. Wang, D. Ren, Y. He, M. Hong, Y. Bai, A. Jia, X. Liu, C. Tang, P. Gong and X. Liu, Tailoring electronic properties and atom utilizations of the Pd species supported on anatase $TiO_2\{101\}$ for efficient CO_2 hydrogenation to formic acid, *ACS Catal.*, 2023, **13**, 10056–10064.

103 H. H. Wang, S. N. Zhang, T. J. Zhao, Y. X. Liu, X. Liu, J. Su, X. H. Li and J. S. Chen, Mild and selective hydrogenation of CO_2 into formic acid over electron-rich MoC nanocatalysts, *Sci. Bull.*, 2020, **65**, 651–657.

104 X. Zhou, Y. Huang, W. Xing, C. Liu, J. Liao and T. Lu, High-quality hydrogen from the catalyzed decomposition of formic acid by Pd–Au/C and Pd–Ag/C, *Chem. Commun.*, 2008, 3540–3542.

105 Z. L. Wang, J. M. Yan, Y. Ping, H. L. Wang, W. T. Zheng and Q. Jiang, An efficient CoAuPd/C catalyst for hydrogen generation from formic acid at room temperature, *Angew. Chem., Int. Ed.*, 2013, **52**, 4406–4409.

106 H. H. Wang, B. Zhang, X. H. Li, M. Antonietti and J. S. Chen, Activating Pd nanoparticles on sol-gel prepared porous g-C_3N_4/SiO_2 via enlarging the Schottky barrier for efficient dehydrogenation of formic acid, *Inorg. Chem. Front.*, 2016, **3**, 1124–1129.

107 A. Zhang, J. Xia, Q. Yao and Z. Lu, Pd–WO_x heterostructures immobilized by MOFs-derived carbon cage for formic acid dehydrogenation, *Appl. Catal., B*, 2022, **309**, 121278.

108 Q. Wang, N. Tsumori, M. Kitta and Q. Xu, Fast dehydrogenation of formic acid over palladium nanoparticles immobilized in nitrogen-doped hierarchically porous carbon, *ACS Catal.*, 2018, **8**, 12041–12045.

109 B. Guo, Q. Li, J. Lin, C. Yu, X. Gao, Y. Fang, Z. Liu, Z. Guo, C. Tang and Y. Huang, Bimetallic AuPd nanoparticles loaded on amine-functionalized porous boron nitride nanofibers for catalytic dehydrogenation of formic acid, *ACS Appl. Nano Mater.*, 2021, **4**, 1849–1857.

110 J. H. Lee, J. Ryu, J. Y. Kim, S. W. Nam, J. H. Han, T. H. Lim, S. Gautam, K. H. Chae and C. W. Yoon, Carbon dioxide mediated, reversible chemical hydrogen storage using a Pd nanocatalyst supported on mesoporous graphitic carbon nitride, *J. Mater. Chem. A*, 2014, **2**, 9490–9495.

111 H. Shen, H. Jin, H. Li, H. Wang, J. Duan, Y. Jiao and S.-Z. Qiao, Acidic CO_2-to-HCOOH electrolysis with industrial-level current on phase engineered tin sulfide, *Nat. Commun.*, 2023, **14**, 2843.

112 X. Han, T. Mou, S. Liu, M. Ji, Q. Gao, Q. He, H. Xin and H. Zhu, Heterostructured Bi-Cu_2S nanocrystals for efficient CO_2 electroreduction to formate, *Nanoscale Horiz.*, 2022, **7**, 508–514.

113 J. Tian, R. Wang, M. Shen, X. Ma, H. Yao, Z. Hua and L. Zhang, Bi-Sn oxides for highly selective CO_2 electroreduction to formate in a wide potential window, *ChemSusChem*, 2021, **14**, 2247–2254.

114 G. Zhang, X. Qin, C. Deng, W. Cai and K. Jiang, Electrocatalytic CO_2 and HCOOH interconversion on Pd-based catalysts, *Adv. Sens. Energy Mater.*, 2022, **1**, 100007.

115 J. Shan, T. Zeng, W. Wu, Y. Tan, N. Cheng and S. Mu, Enhancement of the performance of Pd nanoclusters confined within ultrathin silica layers for formic acid oxidation, *Nanoscale*, 2020, **12**, 12891–12897.

116 X. Zhao, M. Huang, B. Deng, K. Li, F. Li and F. Dong, Interfacial engineering of In_2O_3/InN heterostructure with promoted charge transfer for highly efficient CO_2 reduction to formate, *Chem. Eng. J.*, 2022, **437**, 135114.

117 K. Ye, Z. Zhou, J. Shao, L. Lin, D. Gao, N. Ta, R. Si, G. Wang and X. Bao, In situ reconstruction of a hierarchical Sn–Cu/SnO_x core/shell catalyst for high-performance CO_2 electroreduction, *Angew. Chem., Int. Ed.*, 2020, **59**, 4814–4821.

118 Y. Zhou, Y. Chen, X. Qin, K. Jiang, W. Lin and W. Cai, Boosting electrocatalytic oxidation of formic acid on SnO_2-decorated Pd nanosheets, *J. Catal.*, 2021, **399**, 8–14.

119 S. Liu, X. F. Lu, J. Xiao, X. Wang and X. W. Lou, Bi_2O_3 nanosheets grown on multi-channel carbon matrix to catalyze efficient CO_2 electroreduction to HCOOH, *Angew. Chem., Int. Ed.*, 2019, **58**, 13828–13833.

120 Q. Zhang, M. Sun, C. Y. Yuan, Q. W. Sun, B. Huang, H. Dong and Y. W. Zhang, Strong electronic coupling effects at the heterojunction interface of SnO_2 nanodots and g-C_3N_4 for enhanced CO_2 electroreduction, *ACS Catal.*, 2023, **13**, 7055–7066.

121 Y. Zhu, S. Ding, X. Wang, R. Zhang, X. Feng, X. Sun, G. Xiao and Y. Zhu, Interfacial electronic interaction in In_2O_3/poly(3,4-ethylenedioxythiophene)-modified carbon

heterostructures for enhanced electroreduction of CO_2 to formate, *ACS Appl. Mater. Interfaces*, 2023, **15**, 33633–33642.

122 C. Wang, R. Pang, Z. Pan, Y. Zhu, C. Li, B. Liu and J. Shen, The interfacial aspect of Bi_2O_3/CeO_x heterostructure catalysts for HCOOH production from CO_2 electroreduction, *J. Mater. Chem. A*, 2022, **10**, 22694–22700.

123 Y. X. Duan, Y. T. Zhou, Z. Yu, D. X. Liu, Z. Wen, J. M. Yan and Q. Jiang, Boosting production of HCOOH from CO_2 electroreduction via Bi/CeO_x, *Angew. Chem., Int. Ed.*, 2021, **60**, 8798–8802.

124 X. Feng, H. Zou, R. Zheng, W. Wei, R. Wang, W. Zou, G. Lim, J. Hong, L. Duan and H. Chen, Bi_2O_3/BiO_2 nanoheterojunction for highly efficient electrocatalytic CO_2 reduction to formate, *Nano Lett.*, 2022, **22**, 1656–1664.

125 L. Lu, X. Sun, J. Ma, Q. Zhu, C. Wu, D. Yang and B. Han, Selective electroreduction of carbon dioxide to formic acid on electrodeposited $SnO_2@N$-doped porous carbon catalysts, *Sci. China: Chem.*, 2018, **61**, 228–235.

126 J. Tian, M. Wang, M. Shen, X. Ma, Z. Hua, L. Zhang and J. Shi, Highly efficient and selective CO_2 electro-reduction to hcooh on sn particle-decorated polymeric carbon nitride, *ChemSusChem*, 2020, **13**, 6442–6448.

127 C. He, J. Tao, Y. Ke and Y. Qiu, Graphene-supported small tungsten carbide nanocrystals promoting a Pd catalyst towards formic acid oxidation, *RSC Adv.*, 2015, **5**, 66695–66703.

128 C. Rettenmaier, R. M. Arán Ais, J. Timoshenko, R. N. Rizo, H. S. Jeon, S. Kühl, S. W. Chee, A. Bergmann and B. Roldan Cuenya, Enhanced formic acid oxidation over SnO_2-decorated Pd nanocubes, *ACS Catal.*, 2020, **10**, 14540–14551.

129 S. Sato, T. Arai, T. Morikawa, K. Uemura, T. M. Suzuki, H. Tanaka and T. Kajino, Selective CO_2 conversion to formate conjugated with H_2O oxidation utilizing semiconductor/complex hybrid photocatalysts, *J. Am. Chem. Soc.*, 2011, **133**, 15240–15243.

130 H. Liu, X. Liu, W. Yang, M. Shen, S. Geng, C. Yu, B. Shen and Y. Yu, Photocatalytic dehydrogenation of formic acid promoted by a superior $PdAg@g-C_3N_4$ Mott–Schottky heterojunction, *J. Mater. Chem. A*, 2019, **7**, 2022–2026.

131 Y. Wang, X. Shang, J. Shen, Z. Zhang, D. Wang, J. Lin, J. C. Wu, X. Fu, X. Wang and C. Li, Direct and indirect Z-scheme heterostructure-coupled photosystem enabling cooperation of CO_2 reduction and H_2O oxidation, *Nat. Commun.*, 2020, **11**, 3043.

132 O. Altan, E. Altintas, S. Alemdar and Ö. Metin, The rational design of a graphitic carbon nitride-based dual S-scheme heterojunction with energy storage ability as a day/night photocatalyst for formic acid dehydrogenation, *Chem. Eng. J.*, 2022, **441**, 136047.

133 B. Zhou, J. Song, C. Xie, C. Chen, Q. Qian and B. Han, and Engineering, Mo–Bi–Cd ternary metal chalcogenides: highly efficient photocatalyst for CO_2 reduction to formic acid under visible light, *ACS Sustainable Chem. Eng.*, 2018, **6**, 5754–5759.

134 B. Zhou, X. Kong, S. Vanka, S. Cheng, N. Pant, S. Chu, P. Ghamari, Y. Wang, G. Botton and H. Cuo, A GaN: Sn nanoarchitecture integrated on a silicon platform for converting CO_2 to HCOOH by photoelectrocatalysis, *Energy Environ. Sci.*, 2019, **12**, 2842–2848.

135 Y. Hu, S. Zhang, Z. Zhang, H. Zhou, B. Li, Z. Sun, X. Hu, W. Yang, X. Li and Y. Wang, Enhancing photocatalytic-transfer semi-hydrogenation of alkynes over Pd/C_3N_4 through dual regulation of nitrogen defects and the Mott–Schottky effect, *Adv. Mater.*, 2023, **35**, 2304130.

136 D. Kumar, C. H. Park and C. S. Kim, Robust multimetallic plasmonic core-satellite nanodendrites: highly effective visible-light-induced colloidal CO_2 photoconversion system, *ACS Sustainable Chem. Eng.*, 2018, **6**, 8604–8614.

137 J. He, P. Lyu, B. Jiang, S. Chang, H. Du, J. Zhu and H. Li, A novel amorphous alloy photocatalyst (NiB/In_2O_3) composite for sunlight-induced CO_2 hydrogenation to HCOOH, *Appl. Catal., B*, 2021, **298**, 120603.

138 B. Tang and F. X. Xiao, An overview of solar-driven photoelectrochemical CO_2 conversion to chemical fuels, *ACS Catal.*, 2022, **12**, 9023–9057.

139 J. S. DuChene, G. Tagliabue, A. J. Welch, W. H. Cheng and H. A. Atwater, Hot hole collection and photoelectrochemical CO_2 reduction with plasmonic Au/p-GaN photocathodes, *Nano Lett.*, 2018, **18**, 2545–2550.

140 J. S. DuChene, G. Tagliabue, A. J. Welch, X. Li, W. H. Cheng and H. A. Atwater, Optical excitation of a nanoparticle Cu/p-NiO photocathode improves reaction selectivity for CO_2 reduction in aqueous electrolytes, *Nano Lett.*, 2020, **20**, 2348–2358.

141 M. Halmann, Photoelectrochemical reduction of aqueous carbon dioxide on p-type gallium phosphide in liquid junction solar cells, *Nature*, 1978, **275**, 115–116.

142 C. Li, X. Zhou, Q. Zhang, Y. Xue, Z. Kuang, H. Zhao, C. Mou and H. Chen, Construction of heterostructured $Sn/TiO_2/Si$ photocathode for efficient photoelectrochemical CO_2 reduction, *ChemSusChem*, 2022, **15**, e202200188.

143 M. Kan, Z. W. Yan, X. Wang, J. L. Hitt, L. Xiao, J. M. McNeill, Y. Wang, Y. Zhao and T. E. Mallouk, 2-Aminobenzenethiol-functionalized silver-decorated nanoporous silicon photoelectrodes for selective CO_2 reduction, *Angew. Chem., Int. Ed.*, 2020, **59**, 11462–11469.

144 W. Ma, M. Xie, S. Xie, L. Wei, Y. Cai, Q. Zhang and Y. Wang, Nickel and indium core–shell co-catalysts loaded silicon nanowire arrays for efficient photoelectrocatalytic reduction of CO_2 to formate, *J. Energy Chem.*, 2021, **54**, 422–428.

145 P. Wang, X. Ba, X. Zhang, H. Gao, M. Han, Z. Zhao, X. Chen, L. Wang, X. Diao and G. Wang, Direct Z-scheme heterojunction of $PCN-222/CsPbBr_3$ for boosting photocatalytic CO_2 reduction to HCOOH, *Chem. Eng. J.*, 2023, **457**, 141248.

146 S. Cao, T. Sun, Q. Z. Li, L. Piao and X. Chen, Solar-driven H_2 production from formic acid, *Trends Chem.*, 2023, **5**, 947–960.

147 S. Duan, S. Zhang, S. Chang, S. Meng, Y. Fan, X. Zheng and S. Chen, Efficient photocatalytic hydrogen production

from formic acid on inexpensive and stable phosphide/ $Zn_3In_2S_6$ composite photocatalysts under mild conditions, *Int. J. Hydrogen Energy*, 2019, **44**, 21803–21820.

148 J. Liu, H. Huang, C. Ge, Z. Wang, X. Zhou and Y. Fang, Boosting CdS photocatalytic activity for hydrogen evolution in formic acid solution by P doping and MoS_2 photodeposition, *Nanomaterials*, 2022, **12**, 561.

149 C. Wan, L. Zhou, L. Sun, L. Xu, D. G. Cheng, F. Chen, X. Zhan and Y. Yang, Boosting visible-light-driven hydrogen evolution from formic acid over AgPd/2Dg-C_3N_4 nanosheets Mott–Schottky photocatalyst, *Chem. Eng. J.*, 2020, **396**, 125229.

150 Y. Y. Cai, X. H. Li, Y. N. Zhang, X. Wei, K. X. Wang and J. S. Chen, Highly efficient dehydrogenation of formic acid over a palladium-nanoparticle-based Mott–Schottky photocatalyst, *Angew. Chem., Int. Ed.*, 2013, **52**, 11822–11825.

151 L. Xiao, Y. S. Jun, B. Wu, D. Liu, T. T. Chuong, J. Fan and G. D. Stucky, Carbon nitride supported AgPd alloy nanocatalysts for dehydrogenation of formic acid under visible light, *J. Mater. Chem. A*, 2017, **5**, 6382–6387.

152 H. Issa Hamoud, P. Damacet, D. Fan, N. Assaad, O. I. Lebedev, A. Krystianiak, A. Gouda, O. Heintz, M. Daturi and G. Maurin, Selective photocatalytic dehydrogenation of formic acid by an *in situ*-restructured copper-postmetalated metal–organic framework under visible light, *J. Am. Chem. Soc.*, 2022, **144**, 16433–16446.

153 T. Wang, L. Yang, D. Jiang, H. Cao, A. C. Minja and P. Du, CdS nanorods anchored with crystalline FeP nanoparticles for efficient photocatalytic formic acid dehydrogenation, *ACS Appl. Mater. Interfaces*, 2021, **13**, 23751–23759.

154 H. Cao, T. Wang, A. C. Minja, D. Jiang and P. Du, NiCoP nanoparticles anchored on CdS nanorods for enhanced hydrogen production by visible light-driven formic acid dehydrogenation, *Int. J. Hydrogen Energy*, 2021, **46**, 32435–32444.

155 Q. Yue, Y. Wan, Z. Sun, X. Wu, Y. Yuan and P. Du, MoP is a novel, noble-metal-free cocatalyst for enhanced photocatalytic hydrogen production from water under visible light, *J. Mater. Chem. A*, 2015, **3**, 16941–16947.

156 S. Cao, Y. Chen, H. Wang, J. Chen, X. Shi, H. Li, P. Cheng, X. Liu, M. Liu and L. Piao, Ultrasmall CoP nanoparticles as efficient cocatalysts for photocatalytic formic acid dehydrogenation, *Joule*, 2018, **2**, 549–557.

157 X. Ye, Y. Dong, Z. Zhang, W. Zeng, T. Zhang, F. Liu, X. Guan and L. Guo, Mechanism insights for efficient photocatalytic reforming of formic acid with tunable selectivity: accelerated charges separation and spatially separated active sites, *Appl. Catal., B*, 2023, **338**, 123073.

158 O. Altan and Ö. Metin, Boosting formic acid dehydrogenation via the design of a Z-scheme heterojunction photocatalyst: The case of graphitic carbon nitride/Ag/Ag_3PO_4–AgPd quaternary nanocomposites, *Appl. Surf. Sci.*, 2021, **535**, 147740.